The Journal of Chemical Physics ARTICLE scitation.org/journal/jcp

Time-dependent nuclear-electronic orbital Hartree–Fock theory in a strong uniform magnetic field

Cite as: J. Chem. Phys. 158, 114115 (2023); doi: 10.1063/5.0139675
Submitted: 22 December 2022 • Accepted: 27 February 2023 •
Published Online: 17 March 2023

Tanner Culpitt,[a] Laurens D. M. Peters, Erik I. Tellgren, and Trygve Helgaker

AFFILIATIONS

Hylleraas Centre for Quantum Molecular Sciences, Department of Chemistry, University of Oslo, P.O. Box 1033 Blindern, N-0315 Oslo, Norway

[a]Author to whom correspondence should be addressed: t.p.culpitt@kjemi.uio.no

ABSTRACT

In an ultrastrong magnetic field, with field strength $B \approx B_0 = 2.35 \times 10^5$ T, molecular structure and dynamics differ strongly from that observed on the Earth. Within the Born–Oppenheimer (BO) approximation, for example, frequent (near) crossings of electronic energy surfaces are induced by the field, suggesting that nonadiabatic phenomena and processes may play a more important role in this mixed-field regime than in the weak-field regime on Earth. To understand the chemistry in the mixed regime, it therefore becomes important to explore non-BO methods. In this work, the nuclear-electronic orbital (NEO) method is employed to study protonic vibrational excitation energies in the presence of a strong magnetic field. The NEO generalized Hartree–Fock theory and time-dependent Hartree–Fock (TDHF) theory are derived and implemented, accounting for all terms that result as a consequence of the nonperturbative treatment of molecular systems in a magnetic field. The NEO results for HCN and FHF^- with clamped heavy nuclei are compared against the quadratic eigenvalue problem. Each molecule has three semi-classical modes owing to the hydrogen—two precession modes that are degenerate in the absence of a field and one stretching mode. The NEO-TDHF model is found to perform well; in particular, it automatically captures the screening effects of the electrons on the nuclei, which are quantified through the difference in energy of the precession modes.

I. INTRODUCTION

There has been a recent interest in molecular electronic structure[1–13] and dynamics[14–17] for molecules in a strong magnetic field. The introduction of a magnetic field presents new challenges for the derivation and implementation of quantum-chemical methods. A nonperturbative magnetic treatment of electronic structure requires accounting for additional terms in the electronic Hamiltonian that gives rise to orbital- and spin-Zeeman effects. Additionally, all mathematics and implementation are necessarily complex. For Born–Oppenheimer (BO) molecular dynamics, new terms arise in the nuclear equations of motion due to the magnetic vector potential and geometric vector potential, with the latter being related to a geometric or Berry phase.[18–21] In the context of dynamics, these potentials give rise to the Lorentz force acting on the nuclei as well as a Berry (screening) force,[14–17,22] which is given in terms of the Berry curvature.[14–16,21]

Most methods for studying nonperturbative electronic structure and dynamics in a magnetic field have been developed within the BO paradigm. However, in a strong magnetic field, the ordering of electronic energy levels can change substantially.[23] It is, therefore, plausible that the BO approximation is generally less legitimate in a strong magnetic field than in the field-free case. For this reason, it is desirable to investigate nonperturbative, non-BO electronic structure methods for calculating molecular properties in the presence of a magnetic field. The non-BO theory of molecular systems in a magnetic field has been studied,[24–28] but its general application to molecular systems is not widespread. Recent progress has been made by Adamowicz *et al.*[29–33] by studying the HD molecule beyond the BO approximation in a magnetic field using explicitly correlated Gaussians.

There are several methods for calculating non-BO molecular properties that fall under the umbrella of multicomponent quantum theory,[34–39] where the term "multicomponent" refers to treating more than one type of particle quantum mechanically, all on equal footing. In practice, the central theme of many of these methods is treating both electrons and nuclei quantum mechanically with orbital-based techniques, an idea dating back at least to the

work of Thomas[40] in 1969 and Thomas and Joy[41] in 1970. One such method is the nuclear-electronic orbital (NEO) method, which has historically been used to treat all electrons and selected nuclei (typically protons) quantum mechanically in a molecular system. This approach eliminates the difficulties associated with molecular rotations and translations since the molecular frame is fixed by the clamped nuclei. The NEO method may, thus, be described as "partially" non-BO, representing a compromise between a fully quantum treatment and a partial quantum treatment that can be used to study chemically relevant or interesting quantum effects of certain nuclei.

Research related to the NEO method is ongoing, and in the previous decades, there have been many advances. For wave-function theory, these include the NEO Hartree–Fock (NEO-HF) theory,[42] NEO time-dependent Hartree–Fock (NEO-TDHF) theory,[43] NEO full-configuration-interaction (NEO-FCI) theory,[42] NEO explicitly correlated Hartree–Fock (NEO-XCHF) theory,[44,45] NEO multiconfigurational self-consistent field (NEO-MCSCF) theory,[42] and NEO coupled-cluster (NEO-CC) theory.[46,47] Additionally, there have also been advances in the NEO density-functional theory (NEO-DFT),[48–50] NEO time-dependent density-functional theory (NEO-TDDFT),[43] NEO real-time TDDFT,[51] and molecular dynamics within the NEO framework.[52–54] Finally, a new variant of the NEO method, denoted constrained NEO (cNEO),[55–57] has recently been developed, allowing for the fully quantum treatment of all nuclei by constraining the expectation values of nuclear densities.

Here, we concern ourselves with the development and application of nonperturbative variants of the NEO-HF and NEO-TDHF theories that will be relevant to molecular systems in a strong magnetic field, both methods having been programmed in the software package LONDON.[58] In particular, we are interested in the NEO-TDHF vibrational excitation energies and how they are affected by the introduction of a magnetic field. This has direct relevance to the results obtained using BO molecular dynamics for molecules, including the effects of the Lorentz force and Berry curvature on nuclei. In principle, these effects should be captured directly with the NEO model. To what extent the nuclear Lorentz force will be accurately screened by the electrons within the NEO paradigm is an interesting and open question that we seek to investigate. Toward this end, we examine the HCN and FHF^- molecules, which are both well-known systems in the NEO context, having been extensively studied.[39,43,59,60]

This work is organized as follows: Section II contains the theoretical background and a derivation pertaining to the NEO generalized Hartree–Fock (NEO-GHF) method and a derivation of the generally complex NEO-TDHF working equations. A comparison is made with the results from the quadratic eigenvalue problem (QEP) in a magnetic field. Section III presents the protonic vibrational excitation energies for the HCN and FHF^- molecules as a function of magnetic field strength. A summary of the work and future directions are given in Sec. IV.

II. THEORY

We consider a joint system of N_{nuc} classical/clamped nuclei, N_{p} quantum protons, and N_{el} electrons. We use the notation M_I, Z_I, and $\mathbf{R}_I$ for the mass, atom number, and position of a clamped nucleus I, respectively. We use $\mathbf{r}_i^{\text{e}}$ and $\mathbf{p}_i^{\text{e}}$ for the position operator and canonical momentum operator of electron i, respectively. We use $\mathbf{r}_I^{\text{p}}$ and $\mathbf{p}_I^{\text{p}}$ for the position and canonical-momentum operators of proton I, respectively. The vectors of the collective clamped nuclear, electronic, and protonic coordinates are denoted by $\mathbf{R}$, $\mathbf{r}^{\text{e}}$, and $\mathbf{r}^{\text{p}}$, respectively. The vector potential of a uniform magnetic field $\mathbf{B}$ at position $\mathbf{u}$ is given by $\mathbf{A}(\mathbf{u}) = \frac{1}{2}\mathbf{B} \times (\mathbf{u} - \mathbf{G})$, where $\mathbf{G}$ is the gauge origin.

A. The NEO Hamiltonian in a uniform magnetic field

The nonrelativistic Schrödinger–Pauli Hamiltonian of a molecular system within the NEO framework in a uniform magnetic field comprised of heavy nuclei with quantum protons and electrons can be written as

$$H_{\text{NEO}} = H^{\text{e}} + H^{\text{p}} + V^{\text{ep}} + V^{\text{nuc}}, \tag{1}$$

where we have introduced the electronic Hamiltonian with terms representing the electronic kinetic energy, the repulsion between the electrons, and the attraction of the electrons to the clamped nuclei,

$$H^{\text{e}} = \frac{1}{2m^{\text{e}}}\sum_{i=1}^{N_{\text{el}}}\left[\boldsymbol{\sigma}\cdot\left(\mathbf{p}_i^{\text{e}} - q^{\text{e}}\mathbf{A}(\mathbf{r}_i^{\text{e}})\right)\right]^2 + \sum_{i>j=1}^{N_{\text{el}}}\frac{e^2}{4\pi\varepsilon_0|\mathbf{r}_i^{\text{e}} - \mathbf{r}_j^{\text{e}}|} - \sum_{i=1}^{N_{\text{el}}}\sum_{I=1}^{N_{\text{nuc}}}\frac{Z_I e^2}{4\pi\varepsilon_0|\mathbf{r}_i^{\text{e}} - \mathbf{R}_I|}, \tag{2}$$

the protonic Hamiltonian with similar terms for the protons,

$$H^{\text{p}} = \frac{1}{2m^{\text{p}}}\sum_{I=1}^{N_{\text{p}}}\left[\boldsymbol{\sigma}\cdot\left(\mathbf{p}_I^{\text{p}} - q^{\text{p}}\mathbf{A}(\mathbf{r}_I^{\text{p}})\right)\right]^2 + \sum_{I>J=1}^{N_{\text{p}}}\frac{Z_I Z_I e^2}{4\pi\varepsilon_0|\mathbf{r}_I^{\text{p}} - \mathbf{r}_J^{\text{p}}|} + \sum_{J=1}^{N_{\text{p}}}\sum_{I=1}^{N_{\text{nuc}}}\frac{Z_J Z_I e^2}{4\pi\varepsilon_0|\mathbf{r}_J^{\text{p}} - \mathbf{R}_I|}, \tag{3}$$

the electron–proton attraction operator,

$$V^{\text{ep}} = -\sum_{J=1}^{N_{\text{p}}}\sum_{i=1}^{N_{\text{el}}}\frac{Z_J e^2}{4\pi\varepsilon_0|\mathbf{r}_J^{\text{p}} - \mathbf{r}_i^{\text{e}}|}, \tag{4}$$

and the operator representing the repulsion between the clamped nuclei,

$$V^{\text{nuc}} = \sum_{I>J=1}^{N_{\text{nuc}}}\frac{Z_I Z_J e^2}{4\pi\varepsilon_0|\mathbf{R}_I - \mathbf{R}_J|}. \tag{5}$$

In Eqs. (2)–(5), m^{e} is the electron mass, m^{p} is the proton mass, e is the elementary charge, ε_0 is the vacuum permittivity, $q^{\text{e}} = -e$ is the electron charge, $q^{\text{p}} = e$ is the proton charge, and $\boldsymbol{\sigma}$ is the vector of Pauli matrices,

$$\boldsymbol{\sigma}_x = \begin{pmatrix} 0 & 1 \\ 1 & 0 \end{pmatrix}, \quad \boldsymbol{\sigma}_y = \begin{pmatrix} 0 & -\mathrm{i} \\ \mathrm{i} & 0 \end{pmatrix}, \quad \boldsymbol{\sigma}_z = \begin{pmatrix} 1 & 0 \\ 0 & -1 \end{pmatrix}. \tag{6}$$

In the NEO Born–Oppenheimer approximation, the total ground-state wave function associated with the electrons and quantum protons can be written as the product

$$\Psi(\mathbf{r}^{\text{e}}, \mathbf{r}^{\text{p}}, \mathbf{R}) = \psi^{\text{e}}(\mathbf{r}^{\text{e}}; \mathbf{R})\psi^{\text{p}}(\mathbf{r}^{\text{p}}; \mathbf{R})\Theta(\mathbf{R}), \tag{7}$$

where $\psi^{e}(\mathbf{r}^{e};\ \mathbf{R})$ is the electronic wave function, $\psi^{p}(\mathbf{r}^{p};\ \mathbf{R})$ is the protonic wave function, and $\Theta(\mathbf{R})$ is the wave function for the heavy nuclei. From here onward, we suppress the arguments of the wave functions. Note that the forms of the electronic and protonic kinetic energy operators will require additional terms to enter into the one-particle operators of the Hartree–Fock theory and also necessitate a generally complex implementation in addition to compensation for the gauge-dependence of the Hamiltonian.

B. Quadratic eigenvalue problem

For conventional electronic-structure theory within the BO approximation, the recently developed theory of molecular vibrations in the presence of a magnetic field[61] provides a baseline for a comparison with the NEO-TDHF results. The magnetic field introduces velocity-dependent forces, and the classical equations of motion for the nuclei become

$$m_I\ddot{\mathbf{R}}_I = -\nabla_I V(\mathbf{R}) + q_I\dot{\mathbf{R}}_I \times \mathbf{B} + \sum_J \mathbf{\Omega}_{IJ}^{\mathrm{int}}(\mathbf{R})\,\dot{\mathbf{R}}_J. \tag{8}$$

Here, the first term $-\nabla_I V(\mathbf{R})$ is the BO potential-energy force on nucleus I, the second term $q_I\dot{\mathbf{R}}_I \times \mathbf{B}$ is the (bare) Lorentz force on the nucleus I, while the last term $\sum_J \mathbf{\Omega}_{IJ}^{\mathrm{int}}(\mathbf{R})\dot{\mathbf{R}}_J$ is the Berry force on the nucleus I, expressed in terms of the Berry curvature $\mathbf{\Omega}_{IJ}^{\mathrm{int}}(\mathbf{R})$, whose elements are given by[15,62]

$$\begin{aligned}\Omega_{I\alpha J\beta}^{\mathrm{int}} &= \mathrm{i}\hbar\left[\langle\nabla_{I\alpha}\psi^{e}|\nabla_{J\beta}\psi^{e}\rangle - \langle\nabla_{J\beta}\psi^{e}|\nabla_{I\alpha}\psi^{e}\rangle\right]\\ &= -2\hbar\,\mathrm{Im}\langle\nabla_{I\alpha}\psi^{e}|\nabla_{J\beta}\psi^{e}\rangle,\end{aligned} \tag{9}$$

where $I\alpha$ is a composite nuclear-Cartesian index and $\nabla_{I\alpha}$ differentiates with respect to $R_{I\alpha}$. The Berry force is also referred to as the screening force because it represents the screening (due to the electrons) of the bare Lorentz force acting on the nuclei. Introducing the "external Berry curvature"

$$\Omega_{I\alpha,J\beta}^{\mathrm{ext}} = \delta_{IJ}q_I\epsilon_{\alpha\beta\zeta}B_\zeta, \tag{10}$$

we may write the nuclear equations of motion more compactly as

$$m_I\ddot{\mathbf{R}}_I = -\nabla_I V(\mathbf{R}) + \sum_J \mathbf{\Omega}_{IJ}^{\mathrm{tot}}(\mathbf{R})\,\dot{\mathbf{R}}_J, \tag{11}$$

in terms of the total Berry curvature tensor

$$\mathbf{\Omega}_{IJ}^{\mathrm{tot}}(\mathbf{R}) = \mathbf{\Omega}_{IJ}^{\mathrm{ext}}(\mathbf{R}) + \mathbf{\Omega}_{IJ}^{\mathrm{int}}(\mathbf{R}). \tag{12}$$

Truncating the equation of motion to first order in the displacement $\boldsymbol{\eta} = \mathbf{R} - \mathbf{R}^{\mathrm{eq}}$ from a minimum on the potential energy surface (PES) $V(\mathbf{R}^{\mathrm{eq}})$ and transforming to the frequency domain under the convention that

$$F(\omega) = \int_{-\infty}^{\infty} f(t)\mathrm{e}^{\mathrm{i}\omega t}\,\mathrm{d}t, \tag{13}$$

$$f(t) = \frac{1}{2\pi}\int_{-\infty}^{\infty} F(\omega)\mathrm{e}^{-\mathrm{i}\omega t}\,\mathrm{d}\omega, \tag{14}$$

we obtain

$$\omega^2\, M_I\boldsymbol{\eta}_I(\omega) = \sum_J \mathbf{H}_{IJ}(\mathbf{R}^{\mathrm{eq}})\,\boldsymbol{\eta}_J(\omega) + \mathrm{i}\omega\sum_J \mathbf{\Omega}_{IJ}^{\mathrm{tot}}(\mathbf{R}^{\mathrm{eq}})\,\boldsymbol{\eta}_J(\omega), \tag{15}$$

where the elements of the Hessian matrix at $\mathbf{R}^{\mathrm{eq}}$ are given by

$$H_{I\alpha,J\beta}(\mathbf{R}^{\mathrm{eq}}) = \nabla_{I\alpha}\nabla_{J\beta}V(\mathbf{R})\big|_{\mathbf{R}=\mathbf{R}^{\mathrm{eq}}}. \tag{16}$$

Neglecting the contribution from the total Berry curvature, we recover the usual eigenvalue problem for molecular vibrations, whose eigenvalue is the squared oscillation frequency ω^2. With the Berry curvature included, we have a *quadratic eigenvalue problem (QEP)*,[61,63] which yields the oscillation frequency ω directly rather than ω^2. Note that the external and internal contributions to the total Berry curvature in Eq. (12) may be turned on and off separately, thereby allowing for the investigation of different cases where the Lorentz force or Berry force or both are set to zero in the QEP. For a complete exposition on the QEP, see Ref. 61. For more information on the Berry curvature and molecular dynamics in magnetic fields, see Refs. 15–17 and 62.

C. NEO-GHF theory

Here, we present the equations for the NEO generalized Hartree–Fock (NEO-GHF) theory in a uniform magnetic field. This model subsumes all other spin variants of Hartree–Fock theory, such as unrestricted and restricted Hartree–Fock theories, as the latter two may be derived from the GHF equations by imposing appropriate restrictions on spin.

In what follows, the lowercase (uppercase) p, q, r, and s indices refer to the general electronic (protonic) spinors, the lowercase (uppercase) i, j, k, and l indices refer to the occupied electronic (protonic) spinors, and the lowercase (uppercase) a, b, c, and d indices refer to the virtual electronic (protonic) spinors. Throughout this section, the Greek subscript indices μ, ν, λ, and γ refer to the electronic atomic-orbital (AO) basis, while the Greek subscript indices α, β, χ, and δ refer to the protonic AO basis. The superscript indices τ, κ, ξ, and η all refer to spin, which is to say $\tau, \kappa, \xi, \eta \in \{\uparrow, \downarrow\}$.

A generic spinor is a linear combination of spin-dependent basis functions $\phi(\mathbf{x})$ according to

$$\Phi_i(\mathbf{x}) = \sum_{\mu\tau} c_{\mu i}^{\tau}\phi_\mu^{\tau}(\mathbf{x}), \tag{17}$$

where $\mathbf{x}$ is a mixed space–spin coordinate and each $\phi_\mu^{\tau}(\mathbf{x})$ is the product of a spatial function $\theta_\mu(\mathbf{r})$ and a spin function τ. Thus, for N basis functions, there are $2N$ terms in the sum in Eq. (17) and the Fock and density matrices are blocked $2N \times 2N$ matrices in the AO basis. We adopt the chemists' notation for two-particle integrals over spin-dependent basis functions,

$$\begin{aligned}(\phi_\mu^{\tau}\phi_\nu^{\kappa}|\phi_\lambda^{\xi}\phi_\gamma^{\eta}) &= (\mu^{\tau}\nu^{\kappa}|\lambda^{\xi}\gamma^{\eta})\\ &= \int \mathrm{d}\mathbf{x}_1\mathrm{d}\mathbf{x}_2\phi_\mu^{\tau *}(\mathbf{x}_1)\phi_\nu^{\kappa}(\mathbf{x}_1)r_{12}^{-1}\phi_\lambda^{\xi *}(\mathbf{x}_2)\phi_\gamma^{\eta}(\mathbf{x}_2)\\ &= \int \mathrm{d}\mathbf{r}_1\mathrm{d}\mathbf{r}_2\theta_\mu^{*}(\mathbf{r}_1)\theta_\nu(\mathbf{r}_1)r_{12}^{-1}\theta_\lambda^{*}(\mathbf{r}_2)\theta_\gamma(\mathbf{r}_2)\delta_{\tau\kappa}\delta_{\xi\eta},\end{aligned} \tag{18}$$

and adopt the Coulomb exchange shorthand notation

$$(\mu^{\tau}\nu^{\kappa}\|\lambda^{\xi}\gamma^{\eta}) = (\mu^{\tau}\nu^{\kappa}|\lambda^{\xi}\gamma^{\eta}) - (\mu^{\tau}\gamma^{\eta}|\lambda^{\xi}\nu^{\kappa}). \tag{19}$$

Taking the electronic and protonic wave functions in Eq. (7) to be Slater determinants comprised of spinors, the NEO-GHF energy in a uniform magnetic field becomes

$$E = E^{e} + E^{p} + E^{ep} + V^{\mathrm{nuc}}, \tag{20}$$

where the electronic, protonic, and electronic–protonic energy contributions, respectively, in the AO basis are given by

$$E^{\mathrm{e}} = \sum_{\tau\kappa}\sum_{\mu\nu} D^{\mathrm{e},\kappa\tau}_{\nu\mu} h^{e,\tau\kappa}_{\mu\nu} + \frac{1}{2}\sum_{\tau\kappa\xi\eta}\sum_{\mu\nu\lambda\gamma} D^{\mathrm{e},\kappa\tau}_{\nu\mu} D^{\mathrm{e},\eta\xi}_{\gamma\lambda} (\mu^{\tau}\nu^{\kappa}\|\lambda^{\xi}\gamma^{\eta}) + \frac{1}{2m^{\mathrm{e}}}\sum_{\Upsilon}\sum_{\mu\nu} B_{\Upsilon}\mathcal{S}^{\mathrm{e}}_{\mu\nu}\mathrm{Tr}_{\Sigma}[\boldsymbol{\sigma}_{\Upsilon}\mathbf{D}^{\mathrm{e}}]_{\nu\mu}, \tag{21}$$

$$E^{\mathrm{p}} = \sum_{\tau\kappa}\sum_{\alpha\beta} D^{\mathrm{p},\kappa\tau}_{\beta\alpha} h^{\mathrm{p},\tau\kappa}_{\alpha\beta} + \frac{1}{2}\sum_{\tau\kappa\xi\eta}\sum_{\alpha\beta\chi\delta} D^{\mathrm{p},\kappa\tau}_{\beta\alpha} D^{\mathrm{p},\eta\xi}_{\delta\chi} (\alpha^{\tau}\beta^{\kappa}\|\chi^{\xi}\delta^{\eta}) - \frac{1}{2m^{\mathrm{p}}}\sum_{\Upsilon}\sum_{\alpha\beta} B_{\Upsilon}\mathcal{S}^{\mathrm{p}}_{\alpha\beta}\mathrm{Tr}_{\Sigma}[\boldsymbol{\sigma}_{\Upsilon}\mathbf{D}^{\mathrm{p}}]_{\beta\alpha}, \tag{22}$$

$$E^{\mathrm{ep}} = -\sum_{\tau\kappa\xi\eta}\sum_{\mu\nu}\sum_{\alpha\beta} D^{\mathrm{e},\kappa\tau}_{\nu\mu} D^{\mathrm{p},\eta\xi}_{\beta\alpha} (\mu^{\tau}\nu^{\kappa}|\alpha^{\xi}\beta^{\eta}). \tag{23}$$

In these expressions, Tr_{Σ} denotes the trace over the spin degrees of freedom, $h^{\mathrm{e},\tau\kappa}_{\mu\nu}$ and $h^{\mathrm{p},\tau\kappa}_{\alpha\beta}$ are, respectively, the one-electron and one-proton Hamiltonian matrix elements in the presence of a magnetic field, B_{Υ} is a Cartesian component of the magnetic field vector, $\mathcal{S}^{\mathrm{e}}$ and $\mathcal{S}^{\mathrm{p}}$ are the *purely spatial* electronic and protonic overlap matrices, respectively,

$$\mathcal{S}^{\mathrm{e}}_{\mu\nu} = \int \mathrm{d}\mathbf{r}^{\mathrm{e}}\, \theta^{\mathrm{e}*}_{\mu}(\mathbf{r}^{\mathrm{e}})\theta^{\mathrm{e}}_{\nu}(\mathbf{r}^{\mathrm{e}}), \tag{24}$$

$$\mathcal{S}^{\mathrm{p}}_{\alpha\beta} = \int \mathrm{d}\mathbf{r}^{\mathrm{p}}\, \theta^{\mathrm{p}*}_{\alpha}(\mathbf{r}^{\mathrm{p}})\theta^{\mathrm{p}}_{\beta}(\mathbf{r}^{\mathrm{p}}), \tag{25}$$

while $\mathbf{D}^{\mathrm{e}}$ and $\mathbf{D}^{\mathrm{p}}$ are, respectively, the electronic and protonic spin-blocked density matrices,

$$D^{\mathrm{e},\tau\kappa}_{\mu\nu} = \sum_{i} c^{\mathrm{e},\tau}_{\mu i} c^{\mathrm{e},\kappa*}_{\nu i}, \tag{26}$$

$$D^{\mathrm{p},\tau\kappa}_{\alpha\beta} = \sum_{I} c^{\mathrm{p},\tau}_{\alpha I} c^{\mathrm{p},\kappa*}_{\beta I}. \tag{27}$$

Note that the one-electron and one-proton Hamiltonian matrix elements contain their respective contributions from the canonical momentum, external potential, orbital-Zeeman, and diamagnetic terms.[7,64] The orbital-Zeeman and diamagnetic contributions are due to the presence of the magnetic vector potential in the Hamiltonian, with opposite signs arising from the opposite charges q^{e} and q^{p} in Eq. (1).

Minimization of the energy with respect to the electronic and protonic spinor coefficients under the constraint of orthonormalization of the spinors gives rise to the coupled NEO-GHF Roothaan–Hall equations,

$$\mathbf{F}^{\mathrm{e}}\mathbf{C}^{\mathrm{e}} = \mathbf{S}^{\mathrm{e}}\mathbf{C}^{\mathrm{e}}\boldsymbol{\epsilon}^{\mathrm{e}}, \tag{28}$$

$$\mathbf{F}^{\mathrm{p}}\mathbf{C}^{\mathrm{p}} = \mathbf{S}^{\mathrm{p}}\mathbf{C}^{\mathrm{p}}\boldsymbol{\epsilon}^{\mathrm{p}}, \tag{29}$$

which may be written in spin-blocked form according to

$$\begin{pmatrix} \mathbf{F}^{\mathrm{e},\uparrow\uparrow} & \mathbf{F}^{\mathrm{e},\uparrow\downarrow} \\ \mathbf{F}^{\mathrm{e},\downarrow\uparrow} & \mathbf{F}^{\mathrm{e},\downarrow\downarrow} \end{pmatrix}\begin{pmatrix} \mathbf{c}^{\mathrm{e},\uparrow} \\ \mathbf{c}^{\mathrm{e},\downarrow} \end{pmatrix} = \begin{pmatrix} \mathbf{S}^{\mathrm{e},\uparrow\uparrow} & \mathbf{0} \\ \mathbf{0} & \mathbf{S}^{\mathrm{e},\downarrow\downarrow} \end{pmatrix}\begin{pmatrix} \mathbf{c}^{\mathrm{e},\uparrow} \\ \mathbf{c}^{\mathrm{e},\downarrow} \end{pmatrix}\boldsymbol{\epsilon}^{\mathrm{e}}, \tag{30}$$

$$\begin{pmatrix} \mathbf{F}^{\mathrm{p},\uparrow\uparrow} & \mathbf{F}^{\mathrm{p},\uparrow\downarrow} \\ \mathbf{F}^{\mathrm{p},\downarrow\uparrow} & \mathbf{F}^{\mathrm{p},\downarrow\downarrow} \end{pmatrix}\begin{pmatrix} \mathbf{c}^{\mathrm{p},\uparrow} \\ \mathbf{c}^{\mathrm{p},\downarrow} \end{pmatrix} = \begin{pmatrix} \mathbf{S}^{\mathrm{p},\uparrow\uparrow} & \mathbf{0} \\ \mathbf{0} & \mathbf{S}^{\mathrm{p},\downarrow\downarrow} \end{pmatrix}\begin{pmatrix} \mathbf{c}^{\mathrm{p},\uparrow} \\ \mathbf{c}^{\mathrm{p},\downarrow} \end{pmatrix}\boldsymbol{\epsilon}^{\mathrm{p}}. \tag{31}$$

In these expressions, the spin-blocked overlap matrices are given by

$$S^{\mathrm{e},\tau\kappa}_{\mu\nu} = \int \mathrm{d}\mathbf{x}\, \phi^{\mathrm{e},\tau*}_{\mu}(\mathbf{x})\, \phi^{\mathrm{e},\kappa}_{\nu}(\mathbf{x}), \tag{32}$$

$$S^{\mathrm{p},\tau\kappa}_{\alpha\beta} = \int \mathrm{d}\mathbf{x}\phi^{\mathrm{p},\tau*}_{\alpha}(\mathbf{x})\phi^{\mathrm{p},\kappa}_{\beta}(\mathbf{x}), \tag{33}$$

while the spin-blocked Fock matrices may be written as

$$F^{\mathrm{e},\tau\kappa}_{\mu\nu} = h^{\mathrm{e},\tau\kappa}_{\mu\nu} + G^{\mathrm{ee},\tau\kappa}_{\mu\nu}(\mathbf{D}^{\mathrm{e}}) + G^{\mathrm{ep},\tau\kappa}_{\mu\nu}(\mathbf{D}^{\mathrm{p}}) + {}^{\mathrm{Z}}F^{\mathrm{e},\tau\kappa}_{\mu\nu}, \tag{34}$$

$$F^{\mathrm{p},\tau\kappa}_{\alpha\beta} = h^{\mathrm{p},\tau\kappa}_{\alpha\beta} + G^{\mathrm{pp},\tau\kappa}_{\alpha\beta}(\mathbf{D}^{\mathrm{p}}) + G^{\mathrm{pe},\tau\kappa}_{\alpha\beta}(\mathbf{D}^{\mathrm{e}}) - {}^{\mathrm{Z}}F^{\mathrm{p},\tau\kappa}_{\alpha\beta}, \tag{35}$$

in terms of the two-particle matrix elements

$$G^{\mathrm{ee},\tau\kappa}_{\mu\nu}(\mathbf{D}^{\mathrm{e}}) = \sum_{\xi\eta}\sum_{\lambda\gamma} D^{\mathrm{e},\eta\xi}_{\gamma\lambda}(\mu^{\tau}\nu^{\kappa}\|\lambda^{\xi}\gamma^{\eta}), \tag{36}$$

$$G^{\mathrm{pp},\tau\kappa}_{\alpha\beta}(\mathbf{D}^{\mathrm{p}}) = \sum_{\xi\eta}\sum_{\chi\delta} D^{\mathrm{p},\eta\xi}_{\delta\chi}(\alpha^{\tau}\beta^{\kappa}\|\chi^{\xi}\delta^{\eta}), \tag{37}$$

$$G^{\mathrm{ep},\tau\kappa}_{\mu\nu}(\mathbf{D}^{\mathrm{p}}) = \sum_{\xi\eta}\sum_{\chi\delta} D^{\mathrm{p},\eta\xi}_{\delta\chi}(\mu^{\tau}\nu^{\kappa}|\chi^{\xi}\delta^{\eta}), \tag{38}$$

$$G^{\mathrm{pe},\tau\kappa}_{\alpha\beta}(\mathbf{D}^{e}) = \sum_{\xi\eta}\sum_{\lambda\gamma} D^{\mathrm{e},\eta\xi}_{\gamma\lambda}(\alpha^{\tau}\beta^{\kappa}|\lambda^{\xi}\gamma^{\eta}) \tag{39}$$

and the spin-Zeeman matrix elements

$${}^{\mathrm{Z}}\mathbf{F}^{\mathrm{e}} = \frac{1}{2m^{\mathrm{e}}}\begin{pmatrix} B_z\mathcal{S}^{\mathrm{e}} & (B_x - \mathrm{i}B_y)\mathcal{S}^{\mathrm{e}} \\ (B_x + \mathrm{i}B_y)\mathcal{S}^{\mathrm{e}} & -B_z\mathcal{S}^{\mathrm{e}} \end{pmatrix}, \tag{40}$$

$${}^{\mathrm{Z}}\mathbf{F}^{\mathrm{p}} = \frac{1}{2m^{\mathrm{p}}}\begin{pmatrix} B_z\mathcal{S}^{\mathrm{p}} & (B_x - \mathrm{i}B_y)\mathcal{S}^{\mathrm{p}} \\ (B_x + \mathrm{i}B_y)\mathcal{S}^{\mathrm{p}} & -B_z\mathcal{S}^{\mathrm{p}} \end{pmatrix}. \tag{41}$$

The NEO-GHF equations, along with the NEO-UHF and NEO-RHF special cases, have been implemented in LONDON. The use of London orbitals ensures gauge-origin invariant calculations for the molecular properties, where primitive, unnormalized electronic and protonic London orbitals, respectively, are given by

$$\phi^{\mathrm{e}}_{\mu}(\mathbf{r}^{\mathrm{e}},\mathbf{R}) = \omega^{\mathrm{e}}_{\mu}(\mathbf{r}^{\mathrm{e}},\mathbf{R})\mathrm{e}^{\mathrm{i}q^{\mathrm{e}}\mathbf{A}(\mathbf{R})\cdot\mathbf{r}^{\mathrm{e}}}, \tag{42}$$

$$\phi^{\mathrm{p}}_{\alpha}(\mathbf{r}^{\mathrm{p}},\mathbf{R}) = \omega^{\mathrm{p}}_{\alpha}(\mathbf{r}^{\mathrm{p}},\mathbf{R})\mathrm{e}^{\mathrm{i}q^{\mathrm{p}}\mathbf{A}(\mathbf{R})\cdot\mathbf{r}^{\mathrm{p}}}, \tag{43}$$

where $\omega^{\mathrm{e}}_{\mu}(\mathbf{r}^{\mathrm{e}},\mathbf{R})$ and $\omega^{\mathrm{p}}_{\alpha}(\mathbf{r}^{\mathrm{p}},\mathbf{R})$ are standard primitive Cartesian Gaussian functions. Note the presence of the electronic and protonic charges in Eqs. (42) and (43).

D. Small oscillations in Hartree–Fock theory

Here, we present a derivation of TDHF theory, also known as the random phase approximation (RPA), for the generally complex case, which is applicable in the presence of a magnetic field. The electronic TDHF equations have been derived in various ways, emphasizing either the dynamical aspects[65–67] or that they yield approximations to the static excitation energies[68,69] (see also a recent work explicitly considering magnetic fields[9]). In the present NEO framework, we provide a derivation that emphasizes the analogy with the semiclassical vibrational problem and is valid in the presence of a magnetic field. The NEO-TDHF equations have been previously derived for the purely real-valued case in the absence of a magnetic field.[43]

1. TDHF equations in the time and frequency domains

We determine the time development of the NEO Hartree–Fock wave function by the Dirac–Frenkel variation principle. For a general time-dependent wave function $\psi(t)$ and Hamiltonian H, the Dirac–Frenkel action functional is given by[70]

$$S(\psi) = \int_{t_0}^{t_1} L(\psi, \dot{\psi}, t)\, \mathrm{d}t, \tag{44}$$

where the Lagrangian is

$$L(\psi, \dot{\psi}, t) = \langle \psi(t) | H - \mathrm{i}\partial_t | \psi(t) \rangle. \tag{45}$$

The evolution of the wave function from time t_0 to t_1 is determined by making $S(\Psi)$ stationary with respect to all the variations in Ψ consistent with fixed values at the end points. We parameterize the wave function as

$$|\psi(t)\rangle = \mathrm{e}^{\mathrm{i}\kappa(t)}|0\rangle, \tag{46}$$

where $\kappa(t)$ is the time-dependent Hermitian orbital-rotation operator given by

$$\kappa(t) = \sum_{\bar{P}\bar{Q}} \kappa_{\bar{P}\bar{Q}}(t)\tau_{\bar{P}\bar{Q}}, \quad \tau_{\bar{P}\bar{Q}} = c_{\bar{P}}^\dagger c_{\bar{Q}}, \tag{47}$$

and $|0\rangle$ is a time-independent reference wave function, which is taken to satisfy the conditions

$$\langle 0 | [H, \tau_{\bar{P}\bar{Q}}] | 0 \rangle = 0, \tag{48}$$

for each pair $\bar{P}, \bar{Q}$. With this parameterization, the integrand in the Dirac–Frenkel action functional becomes

$$L(\psi, \dot{\psi}, t) = \langle 0 | \mathrm{e}^{-\mathrm{i}\kappa(t)} (H - \mathrm{i}\partial_t) \mathrm{e}^{\mathrm{i}\kappa(t)} | 0 \rangle. \tag{49}$$

Performing a Baker–Campbell–Hausdorff (BCH) expansion and noting that $[-\mathrm{i}\partial_t, \mathrm{i}\kappa] = \dot{\kappa}$, we arrive at the following expression for the action integrand in terms of $\kappa(t)$ and $\dot{\kappa}(t)$:

$$\begin{aligned} L(\kappa(t), \dot{\kappa}(t)) = {} & \langle 0 | H - \mathrm{i}\partial_t | 0 \rangle + \mathrm{i}\langle 0 | [H, \kappa(t)] - \mathrm{i}\dot{\kappa}(t) | 0 \rangle \\ & - \frac{1}{2}\langle 0 | [[H, \kappa(t)] - \mathrm{i}\dot{\kappa}(t), \kappa(t)] | 0 \rangle + \mathcal{O}(\kappa^3), \end{aligned} \tag{50}$$

where $\langle 0 | - \mathrm{i}\partial_t | 0 \rangle = 0$ since $|0\rangle$ is time independent and $\langle 0 | [H, \kappa] | 0 \rangle = 0$ by Eq. (48). From the requirement that

$$\delta S = \int_{t_0}^{t_1} \delta L(\kappa(t), \dot{\kappa}(t))\, \mathrm{d}t = 0 \tag{51}$$

subject to $\delta\kappa_{\bar{P}\bar{Q}}(t_0) = 0$ and $\delta\kappa_{\bar{P}\bar{Q}}(t_1) = 0$ for each $\delta\kappa_{\bar{P}\bar{Q}}(t)$, we obtain the variational conditions

$$\frac{\partial L(\kappa(t), \dot{\kappa}(t))}{\partial \kappa_{\bar{P}\bar{Q}}(t)} = \frac{\mathrm{d}}{\mathrm{d}t} \frac{\partial L(\kappa(t), \dot{\kappa}(t))}{\partial \dot{\kappa}_{\bar{P}\bar{Q}}(t)}. \tag{52}$$

Inserting the BCH expression in Eq. (50), we obtain for each pair $\bar{P}, \bar{Q}$,

$$\begin{aligned} \mathrm{i}\langle 0 | [\dot{\kappa}(t), \tau_{\bar{P}\bar{Q}}] | 0 \rangle = {} & \frac{1}{2}\langle 0 | [[H, \kappa(t)], \tau_{\bar{P}\bar{Q}}] | 0 \rangle \\ & + \frac{1}{2}\langle 0 | [[H, \tau_{\bar{P}\bar{Q}}], \kappa(t)] | 0 \rangle + \mathcal{O}(\kappa^2). \end{aligned} \tag{53}$$

Using the commutator identity $[A,[B,C]] + [B,[C,A]] + [C,[A,B]] = 0$ and noting that $\langle 0 | [[\tau_{\bar{P}\bar{Q}}, \kappa(t)], H] | 0 \rangle = 0$ by Eq. (48) since $[\tau_{\bar{P}\bar{Q}}, \kappa(t)]$ is a linear combination of excitation operators, we find that

$$\mathrm{i}\langle 0 | [\dot{\kappa}(t), \tau_{\bar{P}\bar{Q}}] | 0 \rangle = \langle 0 | [[H, \kappa(t)], \tau_{\bar{P}\bar{Q}}] | 0 \rangle + \mathcal{O}(\kappa^2(t)), \tag{54}$$

which upon truncation at second order in $\kappa(t)$ gives the TDHF equations in the time domain. Finally, transforming to the frequency domain using the Fourier transform convention in Eq. (13), we arrive at the standard TDHF equations

$$\omega \langle 0 | [\tau_{\bar{P}\bar{Q}}, \hat{\kappa}(\omega)] | 0 \rangle = \langle 0 | [\tau_{\bar{P}\bar{Q}}, [H, \hat{\kappa}(\omega)]] | 0 \rangle, \tag{55}$$

for each pair $\bar{P}, \bar{Q}$.

2. NEO-TDHF equations

Before evaluating Eq. (55), we note that the $\kappa(t)$ operator is restricted to contain only the particle-conserving excitation and de-excitation operators. Additionally, only occupied-virtual excitations and de-excitations are considered. Finally, the Hermiticity of $\kappa(t)$ demands that

$$\begin{aligned} \kappa(t) = {} & \sum_{ia} \kappa_{ai}^{\mathrm{e}}(t) a_a^\dagger a_i + \sum_{ia} \kappa_{ai}^{\mathrm{e}*}(t) a_i^\dagger a_a \\ & + \sum_{IA} \kappa_{AI}^{\mathrm{p}}(t) b_A^\dagger b_I + \sum_{IA} \kappa_{AI}^{\mathrm{p}*}(t) b_I^\dagger b_A, \end{aligned} \tag{56}$$

where we treat $\kappa_{ai}^{\mathrm{e}}(t)$ and $\kappa_{ai}^{\mathrm{e}*}(t)$ and likewise $\kappa_{AI}^{\mathrm{p}}(t)$ and $\kappa_{AI}^{\mathrm{p}*}(t)$ as independent parameters. We may then write the Fourier transforms $\mathcal{F}$ of these functions as

$$\mathcal{F}[\kappa_{ai}^{\mathrm{e}}(t)] = \hat{\kappa}_{ai}^{\mathrm{e}}(\omega) = X_{ai}^{\mathrm{e}}(\omega), \tag{57}$$

$$\mathcal{F}[\kappa_{ai}^{\mathrm{e}*}(t)] = [\hat{\kappa}_{ai}^{\mathrm{e}}(-\omega)]^* = [X_{ai}^{\mathrm{e}}(-\omega)]^* = -Y_{ai}^{\mathrm{e}}(\omega), \tag{58}$$

with analogous equations for the protonic operators. Under the stated constraints, there are four cases to examine,

$$\omega \langle 0 | [a_i^\dagger a_a, \hat{\kappa}(\omega)] | 0 \rangle = \langle 0 | [a_i^\dagger a_a, [H, \hat{\kappa}(\omega)]] | 0 \rangle, \tag{59}$$

$$\omega \langle 0 | [a_a^\dagger a_i, \hat{\kappa}(\omega)] | 0 \rangle = \langle 0 | [a_a^\dagger a_i, [H, \hat{\kappa}(\omega)]] | 0 \rangle, \tag{60}$$

$$\omega \langle 0 | [b_I^\dagger b_A, \hat{\kappa}(\omega)] | 0 \rangle = \langle 0 | [b_I^\dagger b_A, [H, \hat{\kappa}(\omega)]] | 0 \rangle, \tag{61}$$

$$\omega \langle 0 | [b_A^\dagger b_I, \hat{\kappa}(\omega)] | 0 \rangle = \langle 0 | [b_A^\dagger b_I, [H, \hat{\kappa}(\omega)]] | 0 \rangle. \tag{62}$$

Beginning with Eq. (59), we have

$$A^{e}_{ai,bj}X^{e}_{bj} + B^{e}_{ai,bj}Y^{e}_{bj} + T^{e}_{ai,AI}X^{p}_{AI} + R^{e}_{ai,AI}Y^{p}_{AI} = \omega X^{e}_{bj}, \tag{63}$$

where

$$\begin{aligned} A^{e}_{ai,bj} &= \langle 0|[a_i^\dagger a_a, [H, a_b^\dagger a_j]]|0\rangle \\ &= F^{e}_{ab}\delta_{ij} - F^{e}_{ji}\delta_{ab} + (ai\|jb), \end{aligned} \tag{64}$$

$$B^{e}_{ai,bj} = -\langle 0|[a_i^\dagger a_a, [H, a_j^\dagger a_b]]|0\rangle = (ai\|bj), \tag{65}$$

$$T^{e}_{ai,AI} = \langle 0|[a_i^\dagger a_a, [H, b_A^\dagger b_I]]|0\rangle = -(ai|IA), \tag{66}$$

$$R^{e}_{ai,AI} = -\langle 0|[a_i^\dagger a_a, [H, b_I^\dagger b_A]]|0\rangle = -(ai|AI), \tag{67}$$

while Eq. (61) gives the same results, mutatis mutandis, for the protonic case,

$$A^{p}_{AI,BJ}X^{p}_{BJ} + B^{p}_{AI,BJ}Y^{p}_{BJ} + T^{p}_{AI,ai}X^{e}_{ai} + R^{p}_{AI,ai}Y^{e}_{ai} = \omega X^{p}_{BJ}, \tag{68}$$

with

$$\begin{aligned} A^{p}_{AI,BJ} &= \langle 0|[b_I^\dagger b_A, [H, b_B^\dagger b_J]]|0\rangle \\ &= F^{p}_{AB}\delta_{IJ} - F^{p}_{JI}\delta_{AB} + (AI\|JB), \end{aligned} \tag{69}$$

$$B^{p}_{AI,BJ} = -\langle 0|[b_I^\dagger b_A, [H, b_J^\dagger b_B]]|0\rangle = (AI\|BJ), \tag{70}$$

$$T^{p}_{AI,ai} = \langle 0|[b_I^\dagger b_A, [H, a_a^\dagger a_i]]|0\rangle = -(AI|ia), \tag{71}$$

$$R^{p}_{AI,ai} = -\langle 0|[b_I^\dagger b_A, [H, a_i^\dagger a_a]]|0\rangle = -(AI|ai). \tag{72}$$

At this stage, we note that Eq. (60) is equivalent to the conjugate of Eq. (59) followed by the substitution $\omega \to -\omega$, with the same relationship holding for Eqs. (61) and (62). Additionally, it is clear that $\mathbf{T}^{e} = \mathbf{T}^{p\dagger}$ and $\mathbf{R}^{e} = \mathbf{R}^{pT}$, so we need only specify generic "$\mathbf{T}$" and "$\mathbf{R}$" matrices,

$$T_{ai,AI} = -(ai|IA), \tag{73}$$

$$R_{ai,AI} = -(ai|AI). \tag{74}$$

Thus, Eqs. (59)–(62) constitute a generalized eigenvalue problem

$$\begin{pmatrix} \mathbf{A}^{e} & \mathbf{B}^{e} & \mathbf{T} & \mathbf{R} \\ \mathbf{B}^{e*} & \mathbf{A}^{e*} & \mathbf{R}^{*} & \mathbf{T}^{*} \\ \mathbf{T}^{\dagger} & \mathbf{R}^{T} & \mathbf{A}^{p} & \mathbf{B}^{p} \\ \mathbf{R}^{\dagger} & \mathbf{T}^{T} & \mathbf{B}^{p*} & \mathbf{A}^{p*} \end{pmatrix} \begin{pmatrix} \mathbf{X}^{e} \\ \mathbf{Y}^{e} \\ \mathbf{X}^{p} \\ \mathbf{Y}^{p} \end{pmatrix} = \omega \begin{pmatrix} \mathbf{I} & \mathbf{0} & \mathbf{0} & \mathbf{0} \\ \mathbf{0} & -\mathbf{I} & \mathbf{0} & \mathbf{0} \\ \mathbf{0} & \mathbf{0} & \mathbf{I} & \mathbf{0} \\ \mathbf{0} & \mathbf{0} & \mathbf{0} & -\mathbf{I} \end{pmatrix} \begin{pmatrix} \mathbf{X}^{e} \\ \mathbf{Y}^{e} \\ \mathbf{X}^{p} \\ \mathbf{Y}^{p} \end{pmatrix}. \tag{75}$$

In Eq. (75), $\mathbf{X}^{e}$ and $\mathbf{X}^{p}$ are the electronic and protonic excitation amplitudes, respectively; $\mathbf{Y}^{e}$ and $\mathbf{Y}^{p}$ are the electronic and protonic de-excitation amplitudes, respectively; and ω are the eigenvalues, which may be of protonic, electronic, or mixed character. The UHF and RHF variants of Eq. (75) are generated through appropriate restrictions on spin. For the purposes of this work, we are interested in an electronic RHF reference with a single quantum proton. In this specific case, the spin-adaptation of Eq. (75) reveals that only the electronic singlets couple with the protonic excitations. Summation over electronic spin and the variable substitutions $\mathbf{X}^{p} \to \sqrt{2}\mathbf{X}^{p}, \mathbf{Y}^{p} \to \sqrt{2}\mathbf{Y}^{p}$ yield

$$\begin{aligned} &\begin{pmatrix} \mathbf{A}^{e,\sigma} & \mathbf{B}^{e,\sigma} & \sqrt{2}\mathbf{T} & \sqrt{2}\mathbf{R} \\ \mathbf{B}^{e,\sigma*} & \mathbf{A}^{e,\sigma*} & \sqrt{2}\mathbf{R}^{*} & \sqrt{2}\mathbf{T}^{*} \\ \sqrt{2}\mathbf{T}^{\dagger} & \sqrt{2}\mathbf{R}^{T} & \mathbf{A}^{p} & \mathbf{B}^{p} \\ \sqrt{2}\mathbf{R}^{\dagger} & \sqrt{2}\mathbf{T}^{T} & \mathbf{B}^{p*} & \mathbf{A}^{p*} \end{pmatrix} \begin{pmatrix} \mathbf{X}^{e}_{\uparrow} + \mathbf{X}^{e}_{\downarrow} \\ \mathbf{Y}^{e}_{\uparrow} + \mathbf{Y}^{e}_{\downarrow} \\ \sqrt{2}\mathbf{X}^{p}_{\uparrow} \\ \sqrt{2}\mathbf{Y}^{p}_{\uparrow} \end{pmatrix} \\ &= \omega \begin{pmatrix} \mathbf{I} & \mathbf{0} & \mathbf{0} & \mathbf{0} \\ \mathbf{0} & -\mathbf{I} & \mathbf{0} & \mathbf{0} \\ \mathbf{0} & \mathbf{0} & \mathbf{I} & \mathbf{0} \\ \mathbf{0} & \mathbf{0} & \mathbf{0} & -\mathbf{I} \end{pmatrix} \begin{pmatrix} \mathbf{X}^{e}_{\uparrow} + \mathbf{X}^{e}_{\downarrow} \\ \mathbf{Y}^{e}_{\uparrow} + \mathbf{Y}^{e}_{\downarrow} \\ \sqrt{2}\mathbf{X}^{p}_{\uparrow} \\ \sqrt{2}\mathbf{Y}^{p}_{\uparrow} \end{pmatrix}, \end{aligned} \tag{76}$$

where

$$A^{e,\sigma}_{ai,bj} = (\epsilon_a - \epsilon_i)\delta_{ij}\delta_{ab} + 2(ai|jb) - (ab|ji), \tag{77}$$

$$B^{e,\sigma}_{ai,bj} = 2(ai|bj) - (aj|bi), \tag{78}$$

are the spin-adapted singlet variants of their GHF counterparts, written in terms of spin-free orbitals, and $\mathbf{X}^{e}_{\uparrow}$ ($\mathbf{X}^{e}_{\downarrow}$) refers to the spin up (down) excitation amplitudes, with the de-excitations defined analogously. Note that the other blocks $\mathbf{T}, \mathbf{R}, \mathbf{A}^{p}$, and $\mathbf{B}^{p}$ appearing in Eq. (76) are identical in form to their GHF counterparts [see Eqs. (66), (67), (69), and (70)], with the salient difference being that, in the GHF case, the orbitals in question are spinors, while in the spin-adapted case, the orbitals are spin-free.

Finally, as a brief digression on the use of language, we point out that terms such as "mode" are only technically appropriate in their application to the QEP. In NEO-TDHF theory, there are no classical "modes." In Sec. II E, we will demonstrate a scheme for the association of the quantum excitations to their semi-classical counterparts. However, it is to be understood that terms such as "stretching mode" or "precession" in the quantum-mechanical context are used only by analogy to the classical case and do not suggest that the NEO-TDHF case itself is classical.

E. Characterization of NEO-TDHF excitations

In this work, Eq. (76) is solved by inversion of the metric followed by diagonalization. The resulting excitations may be characterized as electronic or protonic according to the dominance of electronic vs protonic amplitudes in the eigenvectors – that is, $\mathbf{X}^{p} \approx \mathbf{0}$ and $\mathbf{Y}^{p} \approx \mathbf{0}$ for an electronic transition, and $\mathbf{X}^{e} \approx \mathbf{0}$ and $\mathbf{Y}^{e} \approx \mathbf{0}$ for a protonic transition.[39,43,60] For the systems studied in this work across all field strengths, the NEO-TDHF excitations of interest remained of dominant protonic character with little fluctuation.

To associate quantum modes with semi-classical modes, we examine the time evolution of the expectation value of the proton position,

$$\langle\psi(t)|\mathbf{r}^{\mathrm{p}}|\psi(t)\rangle = \langle 0|e^{-i\kappa(t)}\,\mathbf{r}^{\mathrm{p}}\,e^{i\kappa(t)}|0\rangle \approx \langle 0|\mathbf{r}^{\mathrm{p}}|0\rangle + \langle 0|[\mathbf{r}^{\mathrm{p}},\, i\kappa(t)]|0\rangle, \tag{79}$$

where we have truncated the BCH expansion at first order in agreement with the stated assumption that $\kappa(t)$ is small. We are interested in the resonances of the Fourier series, which in the TDHF paradigm are taken to be excitation energies. Then, for a particular resonance frequency ω, we have

$$\kappa(t) = \hat{\kappa}(\omega)\,e^{-i\omega t} + \hat{\kappa}(-\omega)\,e^{i\omega t} = \hat{\kappa}(\omega)\,e^{-i\omega t} + \hat{\kappa}(\omega)^*\,e^{i\omega t}. \tag{80}$$

Thus,

$$\langle\psi(t)|\mathbf{r}^{\mathrm{p}}|\psi(t)\rangle = \langle 0|\mathbf{r}^{\mathrm{p}}|0\rangle + i\langle 0|[\mathbf{r}^{\mathrm{p}}, \hat{\kappa}(\omega)]|0\rangle e^{-i\omega t} + \text{c.c.}, \tag{81}$$

where $\langle 0|[\mathbf{r}^{\mathrm{p}}, \hat{\kappa}(\omega)]|0\rangle$ is the transition dipole moment vector,

$$\langle 0|[\mathbf{r}^{\mathrm{p}}, \hat{\kappa}(\omega)]|0\rangle = \sum_{AI}[\langle I|\mathbf{r}^{\mathrm{p}}|A\rangle X^{\mathrm{p}}_{AI} + \langle A|\mathbf{r}^{\mathrm{p}}|I\rangle Y^{\mathrm{p}}_{AI}]. \tag{82}$$

The Fourier component $\boldsymbol{\eta}_{\mathrm{TDHF}}(\omega) = i\langle 0|[\mathbf{r}^{\mathrm{p}}, \hat{\kappa}(\omega)]|0\rangle$ and the time evolution $\boldsymbol{\eta}_{\mathrm{TDHF}}(t) = i\langle 0|[\mathbf{r}^{\mathrm{p}}, \hat{\kappa}(\omega)]|0\rangle e^{-i\omega t} + \text{c.c.}$ may be compared to the corresponding semiclassical quantities obtained from Eq. (15). For the purposes of this work, we are interested in a single quantum proton. In systems where there are multiple quantum protons that can be taken as approximately distinguishable,[71] the procedure outlined above will also be applicable. However, in the general case of multiple quantum protons, $\boldsymbol{\eta}_{\mathrm{TDHF}}(\omega)$ cannot be compared to the QEP due to the indistinguishability of the protons. Other classification metrics will, then, be required, such as spatial symmetry, angular momentum, or density.

Following the same procedure as the expectation value of position, we can examine the time evolution of the density operator

$$n(\mathbf{r}) = n^{\mathrm{e}}(\mathbf{r}) + n^{\mathrm{p}}(\mathbf{r}), \tag{83}$$

where

$$n^{\mathrm{e}}(\mathbf{r}) = \sum_{pq}\Phi^{\mathrm{e}*}_p(\mathbf{r})\Phi^{\mathrm{e}}_q(\mathbf{r})a^\dagger_p a_q, \tag{84}$$

$$n^{\mathrm{p}}(\mathbf{r}) = \sum_{PQ}\Phi^{\mathrm{p}*}_P(\mathbf{r})\Phi^{\mathrm{p}}_Q(\mathbf{r})b^\dagger_P b_Q, \tag{85}$$

and

$$\langle\psi(t)|n(\mathbf{r})|\psi(t)\rangle = \langle 0|n(\mathbf{r})|0\rangle + i\langle 0|[n(\mathbf{r}), \hat{\kappa}(\omega)]|0\rangle e^{-i\omega t} + \text{c.c.} \tag{86}$$

In Eq. (86), $\langle 0|[n(\mathbf{r}), \hat{\kappa}(\omega)]|0\rangle$ is the transition density,

$$\langle 0|[n(\mathbf{r}), \hat{\kappa}(\omega)]|0\rangle = \sum_{ai}[\Phi^{\mathrm{e}*}_i(\mathbf{r})\Phi^{\mathrm{e}}_a(\mathbf{r})X^{\mathrm{e}}_{ai} + \Phi^{\mathrm{e}*}_a(\mathbf{r})\Phi^{\mathrm{e}}_i(\mathbf{r})Y^{\mathrm{e}}_{ai}] + \sum_{AI}[\Phi^{\mathrm{p}*}_I(\mathbf{r})\Phi^{\mathrm{p}}_A(\mathbf{r})X^{\mathrm{p}}_{AI} + \Phi^{\mathrm{p}*}_A(\mathbf{r})\Phi^{\mathrm{p}}_I(\mathbf{r})Y^{\mathrm{p}}_{AI}]. \tag{87}$$

Equations (81) and (82) along with Eqs. (86) and (87) allow for the visualization of the time evolution of the protonic expectation value and total density, respectively, for a given frequency ω. When an excitation is dominated by one type of particle, the other particle's contribution to Eq. (87) can be ignored.

The procedure for associating a given NEO-TDHF mode with a QEP mode is, then, as follows: (1) examine the excitations to find those dominated by protonic amplitudes; (2) compute $\boldsymbol{\eta}_{\mathrm{TDHF}}(t)$ and compare its time evolution to the three QEP modes to find a match (rotation clockwise, rotation counterclockwise, or stretch; see Fig. 1); and (3) compute the time evolution of the density using Eqs. (86) and (87), and ensure that the transition density has a single node, and is of p-type shape.[60] A NEO-TDHF mode that is a counterpart to a QEP mode will fulfill conditions (1), (2), and (3) given above.

In previous studies, transition dipole moment vectors and transition densities were used to interpret the quantum modes calculated with the NEO-TDHF theory.[43,60,71,72] However, this was done only in the frequency domain, where transition dipole moment vectors from NEO calculations were compared with, for example, the normal modes from a harmonic oscillator.[71,72] Additionally, this was done in the absence of a magnetic field, where all quantities could be taken as real valued.

In a magnetic field, the NEO transition dipole moment vectors and transition densities are complex valued. Consequently, it becomes more difficult to understand and interpret these quantities

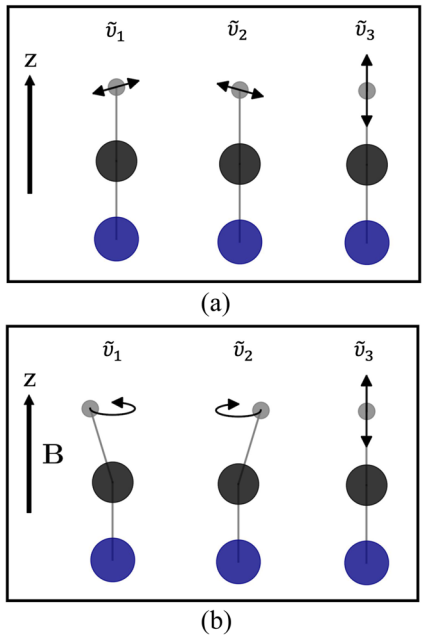

FIG. 1. Schematic representation of protonic vibrational modes of the HCN molecule oriented along the z-axis for clamped C and N nuclei in (a) zero magnetic field and (b) magnetic field oriented along the molecular axis. In panel (a), the two degenerate off-axis bending modes are replaced in panel (b) by non-degenerate precession modes. One precession is counterclockwise, and the other is clockwise. The stretching mode is unaffected by the Lorentz force because its motion is parallel to the field. All depicted modes can be visualized as a function of time using the eigenvectors of the QEP or the transition dipole moment vectors from NEO-TDHF theory as described in the text.

(and express them in the language of semi-classical modes) without recourse to visualization as functions of time. This is why it becomes useful to compute $\boldsymbol{\eta}_{\mathrm{TDHF}}(t)$ as a function of time and the density evolution as a function of time because both of these quantities are real-valued and gauge-independent. We note that the development of real-time NEO methods[51] in a magnetic field may, therefore, be of interest for future investigations.

III. RESULTS

Here, we present the vibrational excitation energies for the hydrogen nuclei of the HCN and FHF^- molecules. Since these molecules have been thoroughly studied in the context of NEO-HF and NEO-TDHF theories in the absence of a magnetic field, they represent a good starting point for discussing the similarities and differences between the field and field-free cases. The heavy nuclei (C, N, and F) of each molecule are clamped, while the hydrogen nucleus and all electrons of each system are treated quantum mechanically with the NEO-TDHF method. Calculations are performed with the LONDON program, for a range of magnetic field strengths, starting from $B = 0$ and ending at $B = B_0 = 2.35 \times 10^5$ T in $0.1B_0$ increments, with the field oriented parallel to the molecular axis in both cases.

All calculations were performed with a singlet electronic NEO-RHF reference configuration and with the proton occupying a spin orbital oriented parallel to the field. The electronic basis set employed in all calculations is a decontracted cc-pVTZ London basis (denoted Lu-cc-pVTZ) for the heavy atoms and a cc-pV5Z basis (denoted Lu-cc-pV5Z) for the hydrogen atom. The protonic basis set used for the hydrogen nuclei is a decontracted London orbital variant of the PB5-F basis set,[73] denoted Lu-PB5-F. Note that the protonic basis set was developed without contraction.[73] It has been shown that, for quantitative results, contracted cc-pV5Z and cc-pV6Z electronic basis sets are required for hydrogen nuclei treated with the NEO method,[43,60] which is why we have chosen to use the decontracted cc-pV5Z basis. The molecular geometries were optimized at each field strength for the conventional electronic case, and the protonic basis functions were placed at the optimized nuclear positions (see the supplementary material for molecular geometries).

For each molecule, there are three protonic vibrational modes: two bending modes perpendicular to the molecular axis and a stretching mode along the molecular axis. The bending modes are degenerate in the absence of a magnetic field. However, once the field is introduced, the degeneracy of these modes is broken by the Lorentz force and the bending modes are then replaced by precessional modes about the field axis—a lower-frequency precession counterclockwise and a higher-frequency precession clockwise. The stretching modes are not split by the field since they lie directly along the field axis. Note that, in the complex-valued case, even zero-field degenerate bending modes can be represented as degenerate precessional modes by taking linear combinations.

In the QEP calculations, the precessional frequencies are affected by the Berry screening force. We consider three cases. The first case, denoted QEP-sL (sL = "screened Lorentz"), is the properly screened scenario, with contributions from both Ω^{int} and Ω^{ext} in Eq. (12). In the second case, denoted QEP-bL (bL = "bare Lorentz"), we set $\Omega^{\mathrm{int}} = 0$, which corresponds to the QEP with only the bare Lorentz force acting on the nuclei. Finally, in the third case, denoted QEP-nL (nL = "no Lorentz"), we set $\Omega^{\mathrm{ext}} = 0$ and $\Omega^{\mathrm{int}} = 0$, corresponding to no Lorentz force at all. These QEP cases are of interest to compare with the NEO-TDHF results because the NEO-TDHF frequencies should inherently contain the effects of Ω^{tot}, including screening. Thus, we expect the NEO-TDHF calculations to match most closely with QEP-sL.

In Fig. 1, the vibrational and precessional modes of HCN are illustrated. In Tables I and II, we have listed the HCN and FHF^-

TABLE I. NEO and QEP precessional ($\tilde{\nu}_1$ and $\tilde{\nu}_2$) and stretching ($\tilde{\nu}_3$) frequencies in units of cm^{-1} for the hydrogen nucleus in HCN as a function of magnetic field strength. All calculations at the Hartree–Fock level of theory as described in the text.

B/B_0	Mode	NEO-TDHF	QEP-sL	QEP-bL	QEP-nL
0.0	$\tilde{\nu}_1$	972	753	753	753
	$\tilde{\nu}_2$	972	753	753	753
	$\tilde{\nu}_3$	3297	3386	3386	3386
0.1	$\tilde{\nu}_1$	979	759	755	761
	$\tilde{\nu}_2$	985	764	767	761
	$\tilde{\nu}_3$	3312	3399	3399	3399
0.2	$\tilde{\nu}_1$	1006	780	773	785
	$\tilde{\nu}_2$	1017	790	797	785
	$\tilde{\nu}_3$	3354	3436	3436	3436
0.3	$\tilde{\nu}_1$	1046	813	803	821
	$\tilde{\nu}_2$	1063	828	839	821
	$\tilde{\nu}_3$	3419	3496	3496	3496
0.4	$\tilde{\nu}_1$	897	604	604	627
	$\tilde{\nu}_2$	945	651	652	627
	$\tilde{\nu}_3$	3543	3617	3617	3617
0.5	$\tilde{\nu}_1$	1082	840	837	867
	$\tilde{\nu}_2$	1137	894	897	867
	$\tilde{\nu}_3$	3650	3717	3717	3717
0.6	$\tilde{\nu}_1$	1257	1038	1032	1068
	$\tilde{\nu}_2$	1319	1098	1104	1068
	$\tilde{\nu}_3$	3763	3823	3823	3823
0.7	$\tilde{\nu}_1$	1426	1217	1209	1250
	$\tilde{\nu}_2$	1495	1285	1293	1250
	$\tilde{\nu}_3$	3878	3930	3930	3930
0.8	$\tilde{\nu}_1$	1591	1387	1377	1424
	$\tilde{\nu}_2$	1668	1462	1472	1424
	$\tilde{\nu}_3$	3995	4038	4038	4038
0.9	$\tilde{\nu}_1$	1752	1552	1540	1593
	$\tilde{\nu}_2$	1837	1634	1647	1593
	$\tilde{\nu}_3$	4111	4144	4144	4144
1.0	$\tilde{\nu}_1$	1911	1716	1701	1760
	$\tilde{\nu}_2$	2003	1805	1820	1760
	$\tilde{\nu}_3$	4226	4248	4248	4248

TABLE II. NEO and QEP precessional ($\tilde{\nu}_1$ and $\tilde{\nu}_2$) and stretching ($\tilde{\nu}_3$) frequencies in units of cm^{-1} for the hydrogen nucleus in FHF^- as a function of magnetic field strength. All calculations at the Hartree–Fock level of theory as described in the text.

B/B_0	Mode	NEO-TDHF	QEP-sL	QEP-bL	QEP-nL
0.0	$\tilde{\nu}_1$	1438	1476	1476	1476
	$\tilde{\nu}_2$	1438	1476	1476	1476
	$\tilde{\nu}_3$	1754	900	900	900
0.1	$\tilde{\nu}_1$	1442	1481	1480	1486
	$\tilde{\nu}_2$	1452	1491	1492	1486
	$\tilde{\nu}_3$	1758	905	905	905
0.2	$\tilde{\nu}_1$	1465	1506	1504	1516
	$\tilde{\nu}_2$	1485	1526	1528	1516
	$\tilde{\nu}_3$	1771	919	919	919
0.3	$\tilde{\nu}_1$	1503	1548	1545	1563
	$\tilde{\nu}_2$	1534	1577	1581	1563
	$\tilde{\nu}_3$	1791	941	941	941
0.4	$\tilde{\nu}_1$	1557	1604	1599	1623
	$\tilde{\nu}_2$	1597	1643	1647	1623
	$\tilde{\nu}_3$	1818	968	968	968
0.5	$\tilde{\nu}_1$	1622	1669	1664	1693
	$\tilde{\nu}_2$	1671	1717	1723	1693
	$\tilde{\nu}_3$	1850	999	999	999
0.6	$\tilde{\nu}_1$	1696	1739	1732	1768
	$\tilde{\nu}_2$	1755	1796	1804	1768
	$\tilde{\nu}_3$	1884	1031	1031	1031
0.7	$\tilde{\nu}_1$	1777	1810	1801	1843
	$\tilde{\nu}_2$	1845	1876	1885	1843
	$\tilde{\nu}_3$	1921	1063	1063	1063
0.8	$\tilde{\nu}_1$	1862	1880	1869	1916
	$\tilde{\nu}_2$	1939	1953	1965	1916
	$\tilde{\nu}_3$	1959	1094	1094	1094
0.9	$\tilde{\nu}_1$	1949	1946	1933	1986
	$\tilde{\nu}_2$	2034	2027	2041	1986
	$\tilde{\nu}_3$	1996	1122	1122	1122
1.0	$\tilde{\nu}_1$	2036	2009	1993	2051
	$\tilde{\nu}_2$	2127	2095	2112	2051
	$\tilde{\nu}_3$	2031	1148	1148	1148

vibrational/precessional frequencies associated with the hydrogen atom for different magnetic field strengths, calculated with the NEO-TDHF and QEP methods. The QEP results are generated with a mass on the order of 10^{24} atomic units for the clamped nuclei.

When comparing NEO and QEP results, we are particularly interested in (1) the magnitudes of the vibrational excitation energies and (2) the magnitude of the splitting of the precessional modes in the screened and unscreened QEP cases. Regarding point (1), a quantitative comparison is not achievable, even in the BO limit, because the QEP neglects all anharmonic effects, which are relevant in both cases, especially so for the FHF^- stretching mode. Nonetheless, qualitative comparisons can be made in the absence of large anharmonic effects. A better general benchmark would be, for example, a grid-based method, such as the Fourier grid Hamiltonian (FGH) method,[74–76] which has previously been used for benchmarking NEO-TDDFT.[43,60] However, a grid-based machinery that fully incorporates the Lorentz force and Berry force is not currently available, although it could be developed in the future. Plots of the harmonic potentials and the potential energy surfaces for FHF^- and HCN at zero field as well as B_0 can be found in the supplementary material.

Regarding point (2), for the chosen orientation of the molecules to the field, it is demonstrated in the Appendix that the absolute value of the frequencies of precessional motion can be calculated according to the simple formula

$$|\omega_\pm| = \sqrt{\frac{\omega_{\rm sc}^2}{4} + \omega_{\rm bend}^2} \mp \frac{\omega_{\rm sc}}{2}, \tag{88}$$

where the two cases correspond to clockwise (ω_-) and counterclockwise (ω_+) precessions about the field axis. Here, $\omega_{\rm bend}$ is the bending frequency as obtained from the PES in the harmonic approximation (QEP-nL), while $\omega_{\rm sc}$ is the screened cyclotron frequency $\omega_{\rm sc} = (q^{\rm P}B_z - \alpha)/m^{\rm P}$, where α is an element of the Berry curvature. In the absence of screening, $\omega_{\rm sc}$ reduces to the standard cyclotron frequency $\omega_{\rm c} = q^{\rm P}B_z/m^{\rm P}$.

The calculated values of $|\omega_\pm|$ exactly reproduce the QEP-bL (using $\omega_{\rm c}$) and QEP-sL (using $\omega_{\rm sc}$) results. Reproduction of the splitting $|\omega_-| - |\omega_+| = \omega_{\rm sc}$ is a particularly robust indicator of capturing the magnetic forces as the splitting only depends on cylindrical symmetry and is independent of $\omega_{\rm bend}$ and the anharmonicity of the PES. This allows for a quantitative comparison of the description of the magnetic effects at the (harmonic) QEP and (anharmonic) NEO levels, respectively. For a derivation of Eq. (88), see the Appendix.

A. HCN

Table I contains the frequencies of the stretching and bending modes of HCN calculated using the NEO-TDHF and QEP methods (all three variants) as functions of the magnetic field strength. The stretching frequency is plotted in Fig. 2, while Fig. 3 shows the bending/precessional frequencies. The stretching frequencies are unaffected by the Lorentz force (by the parallel field orientation of the molecule) and are, therefore, the same for all QEP variants. We note the presence of a discontinuity in the plots, arising from a level crossing between $0.3B_0$ and $0.4B_0$. Examination of the molecular orbitals and the fact that the C–N bond at $0.4B_0$ is significantly longer than it is at $0.3B_0$ indicate that the C–N triple bond is reduced to a single bond and two nonbonding electron pairs at higher field strengths. By using the converged conventional electronic density as an initial guess for the NEO iterations, we were able to converge to the corresponding electronic state in the NEO calculations in this region.

Since HCN contains a terminal hydrogen, we would expect the NEO-TDHF stretching frequency to be lower than the corresponding QEP frequency due to anharmonicity. This is, indeed, observed in Fig. 2, although the difference decreases with increasing field strength as the anharmonicity is affected by a compression of the bond in the field. For the precessional modes, by contrast, the NEO

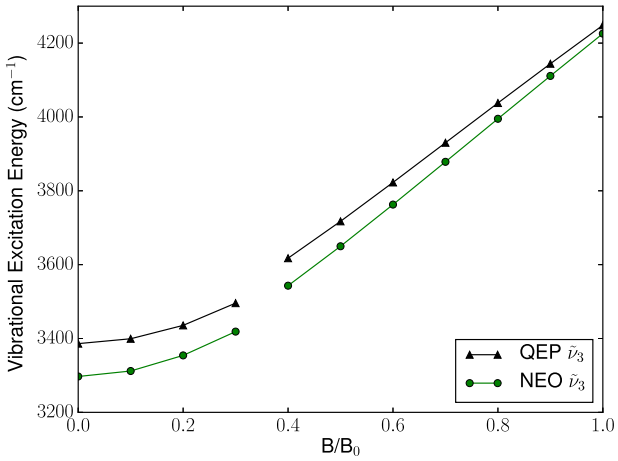

FIG. 2. Vibrational excitation energies corresponding to the stretching mode $\tilde{\nu}_3$ of HCN for the NEO-TDHF and QEP methods. Since the molecule is oriented parallel to the magnetic field, the QEP results are the same for all three variants (QEP-sL = QEP-bL = QEP-nL). The discontinuity in the plot between $0.3B_0$ and $0.4B_0$ is due to a level crossing.

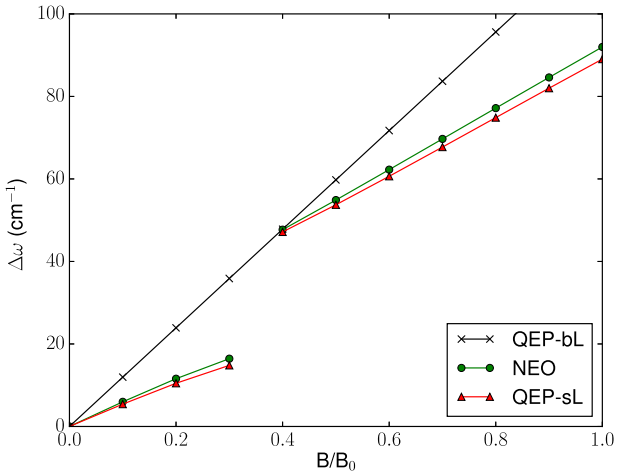

FIG. 4. Difference in energy between the two precessional modes of HCN for the NEO-TDHF, QEP-sL, and QEP-bL methods. For the QEP-bL method, the splitting is equal to the cyclotron frequency for the proton, q^pB_z/m^p. The discontinuity in the plot between $0.3B_0$ and $0.4B_0$ is due to a level crossing.

frequencies are roughly 200 cm^{-1} higher than the QEP frequencies at all field strengths; see Fig. 3. Note that frequencies less than ≈1000 cm^{-1} can be difficult to accurately calculate with NEO-TDHF because of the slow convergence with respect to electronic hydrogen basis set size. The numbers reported here are comparable to previous NEO-TDDFT studies done at zero field for the basis sets employed.[43,60]

An interesting observation in Fig. 3 is that the QEP-bL and QEP-sL calculations do not give the same cyclotron splitting of the precessional modes, as highlighted in the inlay of the figure. This behavior can be understood by noting that the QEP-bL splitting is always equal to the proton's cyclotron frequency, while the QEP-sL splitting vanishes in the limit of perfect screening. As seen in Fig. 4, the NEO splitting agrees well with the QEP-sL results, suggesting that the NEO-TDHF method is capable of capturing the effects of both the bare Lorentz force and the Berry screening force. Note that the effect of the latter greatly decreases at field strengths greater than $0.3B_0$, again reflecting the different character of the ground state in this regime. However, the absence of screening at $0.4B_0$, implied by the fact that the screened and unscreened splittings are nearly identical, might be an artifact of the level of theory in the proximity of an avoided crossing.

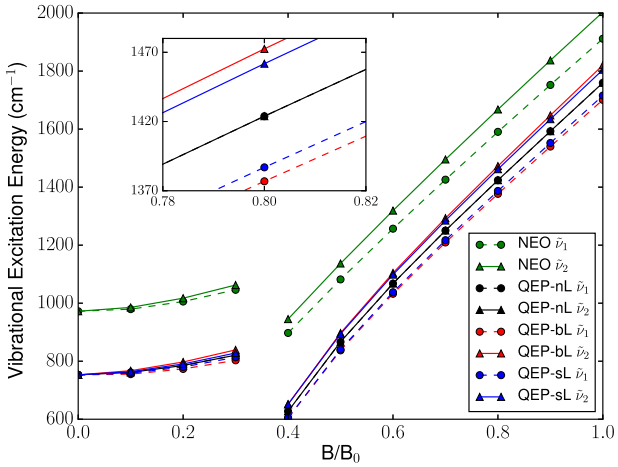

FIG. 3. Vibrational excitation energies corresponding to the precession modes $\tilde{\nu}_1$ and $\tilde{\nu}_2$ of HCN for the NEO-TDHF method and the three variants of the QEP method. The dashed lines with circles correspond to $\tilde{\nu}_1$ for a given method, while the solid lines with triangles correspond to $\tilde{\nu}_2$. The inset highlights the different precessional splittings of the QEP-sL and QEP-bL methods. The discontinuity in the plot between $0.3B_0$ and $0.4B_0$ is due to a level crossing.

B. FHF$^-$

Table II contains the frequencies for the stretching and bending modes of FHF$^-$ calculated using the NEO and QEP methods as functions of magnetic field strength. Figure 5 shows the stretching frequencies, while the bending/precessional frequencies are plotted in Fig. 6. The stretching frequencies are the same for all QEP variants, being unaffected by the Lorentz force due to parallel orientation of molecule to the field.

Previous zero-field studies using DFT and a grid-based FGH method have shown that the stretching frequency of FHF$^-$ is higher than the bending frequencies, in agreement with zero-field NEO-TDDFT results.[43,60] Our field-dependent NEO-TDHF frequencies exhibit the same ordering except in the strongest fields, where the molecule is compressed to the point where one (at $0.9B_0$) or both (at $1.0B_0$) precessional modes become higher in energy than the stretching mode. By contrast, the QEP stretching modes are always lower in energy than the QEP precessional modes. The large difference in magnitude between the QEP and NEO-TDHF stretching mode

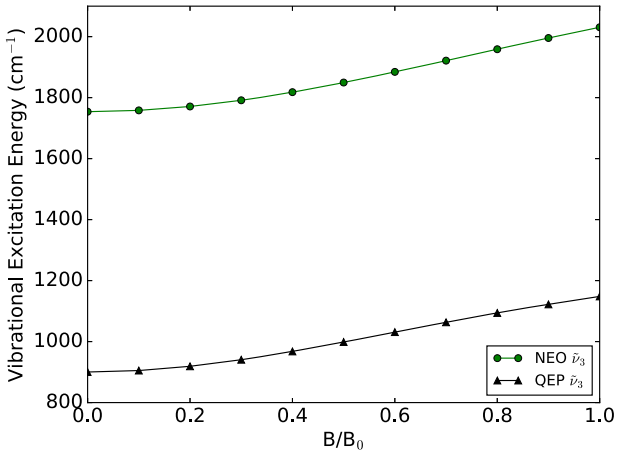

FIG. 5. Vibrational excitation energies corresponding to the stretching mode $\tilde{\nu}_3$ of FHF$^-$ for the NEO-TDHF and QEP methods. Since the molecule is oriented parallel to the magnetic field, the QEP results are the same for all three cases (QEP-sL = QEP-bL = QEP-nL).

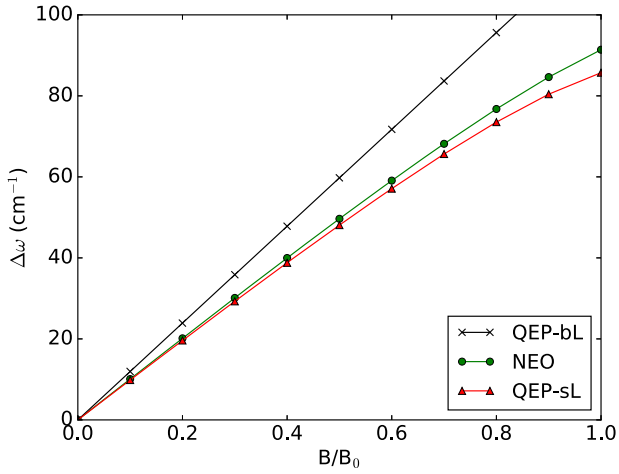

FIG. 7. Difference in energy between the two precessional modes of FHF$^-$ for the NEO-TDHF, QEP-sL, and QEP-bL methods. For the QEP-bL method, the splitting is equal to the cyclotron frequency for the proton, q^pB_z/m^p.

energies (see Fig. 5) is due to considerable anharmonic effects making the bond stiffer relative to the harmonic case; see Fig. S1 in the supplementary material.

In FHF$^-$, the NEO and QEP-sL precessional frequencies are much closer to each other than in HCN, being always less than 100 cm^{-1} apart; see Fig. 6. As was the case for HCN, the cyclotron splitting of the precessional modes is reduced when screening is included by going from the QEP-bL level of theory to the QEP-sL level; see Fig. 7. The NEO-TDHF results again agree very well with the QEP-sL results, demonstrating the capability of the NEO model to directly account for the effects of screening.

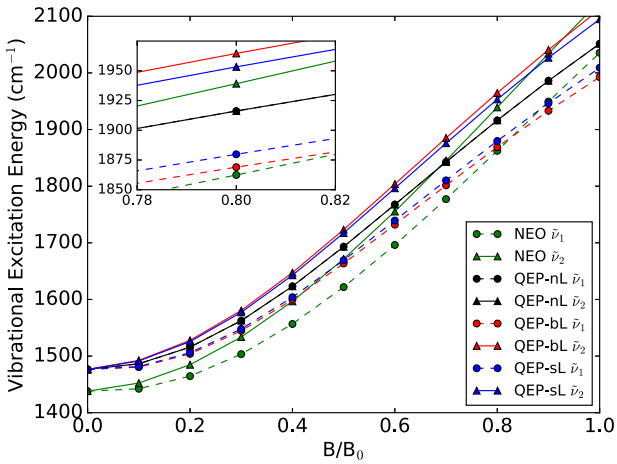

FIG. 6. Vibrational excitation energies corresponding to the precessional modes $\tilde{\nu}_1$ and $\tilde{\nu}_2$ of FHF$^-$ for the NEO-TDHF method and the three variants of the QEP method. The dashed lines with circles correspond to $\tilde{\nu}_1$ for a given method, while the solid lines with triangles correspond to $\tilde{\nu}_2$. The inset highlights the different precessional splittings of the QEP-sL and QEP-bL methods.

IV. CONCLUSIONS

In this work, we have presented the theory and implementation of the NEO-GHF and NEO-TDHF models in the presence of a uniform magnetic field. The NEO-TDHF derivation proceeded through the Dirac–Frenkel action. For a given transition, the protonic position expectation value and density as a function of time can be visualized, aiding in the characterization of the excitations. The relevant equations were implemented in the London program, which utilizes London orbitals for gauge-origin invariant calculations in a magnetic field.

The NEO-TDHF results for the precessional and stretching modes of the HCN and FHF$^-$ molecules were compared to the QEP results for three cases: QEP-nL (no Lorentz forces), QEP-bL (bare Lorentz forces, and QEP-sL (screened Lorentz forces). Because the QEP-sL model includes the screened Lorentz force, it is the most appropriate QEP variant for comparison with the NEO method. The NEO excitation energies were found to be within ≈200 cm^{-1} of the QEP-sL energies except for the FHF$^-$ stretching mode, which showed a larger disparity, likely due to anharmonic effects. These differences are comparable to those observed in the zero-field case.

The degeneracy of the precessional (bending) mode is lifted in a magnetic field by coupling to the cyclotron motion. The precessional splitting is independent of the PES in both the screened and bare Lorentz cases, allowing for quantitative comparisons of the NEO and QEP results. The QEP-bL splitting is always greater than the QEP-sL and NEO splittings, in agreement with the observation that degeneracy is recovered in the limit of perfect screening. The QEP-sL and NEO splittings are in excellent agreement, confirming that the NEO model directly accounts for the effects of the Berry curvature.

The capability of NEO-TDHF to account for screening of the Lorentz force is significant, bearing in mind that the QEP-sL model requires the Berry curvature to be evaluated, making this model much more complex and expensive than the QEP-nL and QEP-bL

models. By contrast, the NEO-TDHF model includes Lorentz screening automatically, in addition to non-BO and nuclear quantum effects. In our examples, these effects tend to reduce the screening experienced by hydrogen in the field with respect to the BO treatment.

One drawback of NEO-TDHF currently is that in order to ensure accurate protonic excitation energies, the electronic hydrogen atom basis sets need to be large.[43,60] However, having numerically verified that NEO-TDHF captures the effects of Berry curvature and splitting of modes for the systems studied, we conclude that NEO-TDHF, in principle, captures all the effects that the QEP captures. As NEO-TDHF additionally captures anharmonicity and non-BO effects, it is the more accurate of the methods. Therefore, the future development of NEO methods in a magnetic field will be of interest, especially so for molecular dynamics, where screening is of great importance.

SUPPLEMENTARY MATERIAL

See the supplementary material for HCN and FHF^- geometries and plots of the harmonic potentials and the potential energy surfaces for FHF^- and HCN at zero field and B_0.

ACKNOWLEDGMENTS

This work was supported by the Research Council of Norway through "Magnetic Chemistry" Grant No. 287950 and CoE Hylleraas Centre for Quantum Molecular Sciences Grant No. 262695. The work also received support from the UNINETT Sigma2, the National Infrastructure for High Performance Computing and Data Storage, through a grant of computer time (Grant No. NN4654K).

AUTHOR DECLARATIONS

Conflict of Interest

The authors have no conflicts to disclose.

Author Contributions

Tanner Culpitt: Conceptualization (lead); Formal analysis (lead); Investigation (lead); Software (lead); Writing – original draft (lead); Writing – review & editing (lead). **Laurens D. M. Peters**: Formal analysis (equal); Investigation (equal); Software (supporting); Writing – original draft (equal); Writing – review & editing (equal). **Erik I. Tellgren**: Formal analysis (equal); Investigation (equal); Software (supporting); Writing – original draft (equal); Writing – review & editing (equal). **Trygve Helgaker**: Formal analysis (equal); Funding acquisition (lead); Investigation (equal); Resources (lead); Writing – original draft (equal); Writing – review & editing (equal).

DATA AVAILABILITY

The data that support the findings of this study are available within the article.

APPENDIX: BENDING VIBRATION AND PRECESSION FOR A CYLINDRICALLY SYMMETRIC MODEL SYSTEM

Consider a molecule with a linear equilibrium structure. We take the molecule to be aligned to the z-axis, with N nuclear positions at $\mathbf{r}_j = (0, 0, z_j)$, labeled in the order of decreasing coordinate $z_j > z_{j+1}$ with $j = 1, \ldots, N$. Furthermore, we assume that the molecule has a bending mode that involves only the first atom located at one end and the other nuclei being clamped. We fix the bond distance $R = |z_1 - z_2|$ and assume cylindrical symmetry around the z-axis. We take into account the forces from the electronic PES and the bare Lorentz force and the Berry screening force. With the spherical coordinate system defined as in Fig. 8, the nuclear position and magnetic field are given by

$$\mathbf{r}_1 = \begin{pmatrix} R\sin(\theta)\cos(\phi) \\ R\sin(\theta)\sin(\phi) \\ R\cos(\theta) \end{pmatrix}, \quad \mathbf{B} = \begin{pmatrix} 0 \\ 0 \\ B_z \end{pmatrix}. \tag{A1}$$

The potential is taken to be a function $V(\theta)$ of θ, while the magnetic forces are taken to be described by a vector potential that depends on θ in the manner

$$\mathbf{a}_1(\theta) = \frac{1}{2}\mathbf{B} \times \mathbf{r}_1 = \frac{1}{2}B_z R\sin(\theta)\mathbf{e}_\phi. \tag{A2}$$

Because we are solely interested in the motion of the nucleus at $\mathbf{r}_1$, we need only consider the screening force that arises from the Berry curvature at that nucleus [see Eq. (8)], corresponding to a single $I = J$ block of Eq. (9). The Berry screening force, then, becomes

$$\boldsymbol{\Omega}(\mathbf{r})\dot{\mathbf{r}}_1 = \mathbf{s}_1(\mathbf{r}) \times \dot{\mathbf{r}}_1, \tag{A3}$$

where $\mathbf{s}_1$ is the curl of the corresponding geometric vector potential,

$$\mathbf{s}_1(\mathbf{r}) = \nabla \times \boldsymbol{\chi}_1(\mathbf{r}), \quad \boldsymbol{\chi}_1(\mathbf{r}) = \langle\psi|\mathbf{p}_1|\psi\rangle. \tag{A4}$$

Here, ψ is the electronic wave function and $\mathbf{p}_1 = -\mathrm{i}\frac{\partial}{\partial \mathbf{r}_1}$ is the canonical momentum operator for the nucleus at $\mathbf{r}_1$. Note that $\mathbf{s}_1(\mathbf{r})$ and $\boldsymbol{\chi}_1(\mathbf{r})$ are functions of the coordinates of all nuclei because they depend on the electronic wave function of the entire system. In a molecule, the screening force generated by Eq. (A3) will, therefore, in general, not be complete (i.e., exactly canceling the bare Lorentz force), as it would for an atom undergoing similar motion.[15]

For the given orientation of the molecule to the field, $\mathbf{s}_1(\mathbf{r})$ has only a nonzero z component.[15] We now make the additional assumption that, for small deviations of θ and ϕ around equilibrium, $\mathbf{s}_1(\mathbf{r})$ is constant,

$$\mathbf{s}_1(\mathbf{r}) = \begin{pmatrix} 0 \\ 0 \\ \alpha \end{pmatrix}. \tag{A5}$$

Under this assumption, we can represent the geometric vector potential in the symmetric gauge, analogous to the magnetic vector potential in Eq. (A2):

$$\boldsymbol{\chi}_1(\theta) = \frac{1}{2}\mathbf{s}_1 \times \mathbf{r}_1 = \frac{1}{2}\alpha R\sin(\theta)\mathbf{e}_\phi. \tag{A6}$$

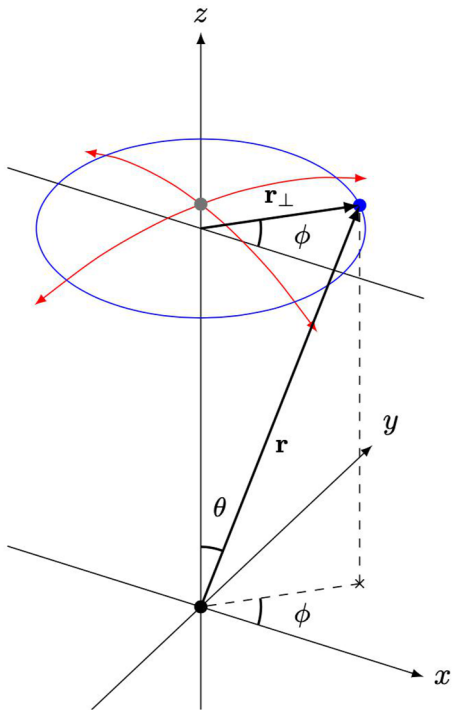

FIG. 8. Spherical coordinate system. The bending modes and precession modes are illustrated, respectively, in red and blue for a triatomic linear molecule.

The Lagrangian consists of one contribution identical to a three-dimensional pendulum, along with magnetic and geometric vector potentials

$$\begin{aligned}\mathcal{L} &= \frac{m}{2}\dot{\mathbf{r}}_1^2 + \dot{\mathbf{r}}_1 \cdot [q\mathbf{a}_1(\theta) - \boldsymbol{\chi}_1(\theta)] - V(\theta) \\ &= \frac{1}{2}mR^2\dot{\theta}^2 + \frac{1}{2}mR^2(\dot{\phi}^2 + \omega_{\rm sc}\dot{\phi})\sin(\theta)^2 - V(\theta),\end{aligned} \tag{A7}$$

where the screened cyclotron frequency,

$$\omega_{\rm sc} = \frac{qB_z - \alpha}{m}, \tag{A8}$$

is calculated from the effective magnetic field B_z and a screening contribution α. In the absence of screening, $\alpha = 0$, we recover the standard cyclotron frequency $\omega_c = qB_z/m$. Calculating the generalized momenta, we obtain

$$p_\theta = \frac{\partial \mathcal{L}}{\partial \dot{\theta}} = mR^2\dot{\theta}, \tag{A9}$$

$$p_\phi = \frac{\partial \mathcal{L}}{\partial \dot{\phi}} = mR^2(\dot{\phi} + \frac{1}{2}\omega_{\rm sc})\sin(\theta)^2, \tag{A10}$$

while the generalized forces are given by

$$F_\theta = \frac{\partial \mathcal{L}}{\partial \theta} = mR^2(\dot{\phi}^2 + \omega_{\rm sc}\dot{\phi})\sin(\theta)\cos(\theta) - \frac{\partial V}{\partial \theta}, \tag{A11}$$

$$F_\phi = \frac{\partial \mathcal{L}}{\partial \phi} = 0. \tag{A12}$$

We will solve Lagrange's equations of motion $\dot{p}_\theta = F_\theta$ and $\dot{p}_\phi = F_\phi$ in two special cases: for a *pure bending motion* with constant ϕ and varying θ and for a *pure precessional motion* with constant angular velocity $\dot{\phi}$ and constant θ.

We consider the bending motion first. Since $F_\phi = 0$, the equation of motion for ϕ becomes $\dot{p}_\phi = 0$, implying that the momentum is conserved,

$$p_\phi = mR^2\left(\dot{\phi} + \frac{1}{2}\omega_{\rm sc}\right)\sin(\theta)^2 = C. \tag{A13}$$

A pure bending mode, with constant ϕ and varying θ, is, therefore, possible only if $\omega_{\rm sc} = 0$. From Eq. (A8), we see that this happens either in a zero magnetic field where $qB_z = \alpha = 0$ or in a magnetic field with perfect screening $qB_z = \alpha$. In the harmonic approximation, $V(\theta) = \frac{1}{2}k\theta^2$, Lagrange's equation of motion $\dot{p}_\theta = F_\theta$, then, simplifies to

$$mR^2\ddot{\theta} + k\theta = 0. \tag{A14}$$

Introducing the vibrational frequency

$$\omega_{\rm bend} = \sqrt{\frac{k}{mR^2}}, \tag{A15}$$

we may write the solution as $\theta(t) = \theta_0 \sin(\omega_{\rm bend}t + \alpha_0)$, where α_0 is a constant.

A pure precessional motion corresponds to constant $\dot{\phi}$ and constant θ and, therefore, $\dot{\theta} = 0$. The latter condition is possible if and only if $F_\theta = 0$ vanishes, yielding a quadratic equation for $\dot{\phi}$,

$$\dot{\phi}^2 + \omega_{\rm sc}\dot{\phi} - \frac{\partial V/\partial\theta}{mR^2\sin(\theta)\cos(\theta)} = 0. \tag{A16}$$

In the harmonic approximation $V(\theta) \approx \frac{1}{2}k\theta^2$ with a sufficiently small value of θ so that $\sin(\theta) \approx \theta$ and $\cos(\theta) \approx 1$, we obtain the solutions

$$\dot{\phi}_\pm \approx -\frac{\omega_{\rm sc}}{2} \pm \sqrt{\frac{\omega_{\rm sc}^2}{4} + \omega_{\rm bend}^2}. \tag{A17}$$

Hence, the two possible precessional frequencies may be predicted from the effective cyclotron frequency (with or without screening) and the bending frequency. To demonstrate the accuracy of the outlined derivation, calculation of the magnitude of the two precessional frequencies according to Eq. (A17) using only $\omega_{\rm bend}$, B_z, and α as inputs yields exactly the same results as QEP-bL ($\alpha = 0$) and QEP-sL.

Finally, we remark that the precessional motion in the Cartesian coordinates takes the form

$$\mathbf{r}_1 = R\begin{pmatrix}\sin(\theta)\cos(\dot{\phi}_\pm t)\\ \sin(\theta)\sin(\dot{\phi}_\pm t)\\ \cos(\theta)\end{pmatrix}, \tag{A18}$$

where θ and $\dot{\phi}_\pm$ are constant. Because $2\cos(\dot{\phi}_\pm t) = e^{i\dot{\phi}_\pm t} + e^{-i\dot{\phi}_\pm t}$ and $2i\sin(\dot{\phi}_\pm t) = e^{i\dot{\phi}_\pm t} - e^{-i\dot{\phi}_\pm t}$, the Fourier spectrum of this motion has the frequencies $\pm\dot{\phi}_\pm$. When the motion is analyzed in Fourier space, we, thus, obtain a total of four frequencies for the two possible precessional motions. Among these frequencies, we may, for example, calculate

$$(-\dot{\phi}_-) - \dot{\phi}_+ = |\dot{\phi}_-| - |\dot{\phi}_+| = \omega_{sc}, \tag{A19}$$

which corresponds to the difference in excitation energies $|\dot{\phi}_-|$ and $|\dot{\phi}_+|$. This quantity has the virtue of being insensitive to the potential energy surface $V(\theta)$ as long as it is cylindrically symmetric.

REFERENCES

[1] K. K. Lange, E. I. Tellgren, M. R. Hoffmann, and T. Helgaker, Science **337**, 327 (2012).
[2] E. I. Tellgren, S. S. Reine, and T. Helgaker, Phys. Chem. Chem. Phys. **14**, 9492 (2012).
[3] S. Stopkowicz, J. Gauss, K. K. Lange, E. I. Tellgren, and T. Helgaker, J. Chem. Phys. **143**, 074110 (2015).
[4] J. W. Furness, J. Verbeke, E. I. Tellgren, S. Stopkowicz, U. Ekström, T. Helgaker, and A. M. Teale, J. Chem. Theory Comput. **11**, 4169 (2015).
[5] F. Hampe and S. Stopkowicz, J. Chem. Phys. **146**, 154105 (2017).
[6] S. Stopkowicz, Int. J. Quantum Chem. **118**, e25391 (2018).
[7] S. Sun, D. B. Williams-Young, T. F. Stetina, and X. Li, J. Chem. Theory Comput. **15**, 348 (2019).
[8] F. Hampe and S. Stopkowicz, J. Chem. Theory Comput. **15**, 4036 (2019).
[9] S. Sen, K. K. Lange, and E. I. Tellgren, J. Chem. Theory Comput. **15**, 3974 (2019).
[10] F. Hampe, N. Gross, and S. Stopkowicz, Phys. Chem. Chem. Phys. **22**, 23522 (2020).
[11] T. J. P. Irons, G. David, and A. M. Teale, J. Chem. Theory Comput. **17**, 2166 (2021).
[12] M. Wibowo, T. J. P. Irons, and A. M. Teale, J. Chem. Theory Comput. **17**, 2137 (2021).
[13] G. David, T. J. P. Irons, A. E. A. Fouda, J. W. Furness, and A. M. Teale, J. Chem. Theory Comput. **17**, 5492 (2021).
[14] D. Ceresoli, R. Marchetti, and E. Tosatti, Phys. Rev. B **75**, 161101 (2007).
[15] T. Culpitt, L. D. M. Peters, E. I. Tellgren, and T. Helgaker, J. Chem. Phys. **155**, 024104 (2021).
[16] L. D. M. Peters, T. Culpitt, L. Monzel, E. I. Tellgren, and T. Helgaker, J. Chem. Phys. **155**, 024105 (2021).
[17] L. Monzel, A. Pausch, L. D. M. Peters, E. I. Tellgren, T. Helgaker, and W. Klopper, J. Chem. Phys. **157**, 054106 (2022).
[18] M. V. Berry, Proc. R. Soc. London, Ser. A **392**, 45 (1984).
[19] C. A. Mead, Rev. Mod. Phys. **64**, 51 (1992).
[20] J. Anandan, J. Christian, and K. Wanelik, Am. J. Phys. **65**, 180 (1997).
[21] R. Resta, J. Phys.: Condens. Matter **12**, R107 (2000).
[22] X. Bian, T. Qiu, J. Chen, and J. E. Subotnik, J. Chem. Phys. **156**, 234107 (2022).
[23] G. Wunner and H. Ruder, Phys. Scr. **36**, 291 (1987).
[24] J. E. Avron, I. W. Herbst, and B. Simon, Ann. Phys. **114**, 431 (1978).
[25] P. Schmelcher, L. S. Cederbaum, and H.-D. Meyer, Phys. Rev. A **38**, 6066 (1988).
[26] P. Schmelcher, L. S. Cederbaum, and H.-D. Meyer, J. Phys. B: At., Mol. Opt. Phys. **21**, L445 (1988).
[27] T. Detmer, P. Schmelcher, and L. S. Cederbaum, J. Phys. B: At., Mol. Opt. Phys. **28**, 2903 (1995).
[28] P. Schmelcher and L. S. Cederbaum, Int. J. Quantum Chem. **64**, 501 (1997).
[29] L. Adamowicz, E. I. Tellgren, and T. Helgaker, Chem. Phys. Lett. **639**, 295 (2015).
[30] L. Adamowicz, M. Stanke, E. Tellgren, and T. Helgaker, Chem. Phys. Lett. **682**, 87 (2017).
[31] L. Adamowicz, M. Stanke, E. Tellgren, and T. Helgaker, J. Chem. Phys. **149**, 244112 (2018).
[32] L. Adamowicz, M. Stanke, E. Tellgren, and T. Helgaker, Chem. Phys. Lett. **761**, 138041 (2020).
[33] L. Adamowicz, S. Kvaal, C. Lasser, and T. B. Pedersen, J. Chem. Phys. **157**, 144302 (2022).
[34] T. Kreibich and E. K. U. Gross, Phys. Rev. Lett. **86**, 2984 (2001).
[35] A. D. Bochevarov, E. F. Valeev, and C. D. SheRrill, Mol. Phys. **102**, 111 (2004).
[36] H. Nakai, Int. J. Quantum Chem. **107**, 2849 (2007).
[37] T. Ishimoto, M. Tachikawa, and U. Nagashima, Int. J. Quantum Chem. **109**, 2677 (2009).
[38] A. Reyes, F. Moncada, and J. Charry, Int. J. Quantum Chem. **119**, e25705 (2019).
[39] F. Pavošević, T. Culpitt, and S. Hammes-Schiffer, Chem. Rev. **120**, 4222 (2020).
[40] I. L. Thomas, Phys. Rev. **185**, 90 (1969).
[41] I. L. Thomas and H. W. Joy, Phys. Rev. A **2**, 1200 (1970).
[42] S. P. Webb, T. Iordanov, and S. Hammes-Schiffer, J. Chem. Phys. **117**, 4106 (2002).
[43] Y. Yang, T. Culpitt, and S. Hammes-Schiffer, J. Phys. Chem. Lett. **9**, 1765 (2018).
[44] C. Swalina, M. V. Pak, A. Chakraborty, and S. Hammes-Schiffer, J. Phys. Chem. A **110**, 9983 (2006).
[45] A. Sirjoosingh, M. V. Pak, C. Swalina, and S. Hammes-Schiffer, J. Chem. Phys. **139**, 034102 (2013).
[46] F. Pavošević, T. Culpitt, and S. Hammes-Schiffer, J. Chem. Theory Comput. **15**, 338 (2019).
[47] F. Pavošević and S. Hammes-Schiffer, J. Chem. Phys. **150**, 161102 (2019).
[48] Y. Yang, K. R. Brorsen, T. Culpitt, M. V. Pak, and S. Hammes-Schiffer, J. Chem. Phys. **147**, 114113 (2017).
[49] K. R. Brorsen, Y. Yang, and S. Hammes-Schiffer, J. Phys. Chem. Lett. **8**, 3488 (2017).
[50] Z. Tao, Y. Yang, and S. Hammes-Schiffer, J. Chem. Phys. **151**, 124102 (2019).
[51] L. Zhao, Z. Tao, F. Pavošević, A. Wildman, S. Hammes-Schiffer, and X. Li, J. Phys. Chem. Lett. **11**, 4052 (2020).
[52] L. Zhao, A. Wildman, Z. Tao, P. Schneider, S. Hammes-Schiffer, and X. Li, J. Chem. Phys. **153**, 224111 (2020).
[53] L. Zhao, A. Wildman, F. Pavošević, J. C. Tully, S. Hammes-Schiffer, and X. Li, J. Phys. Chem. Lett. **12**, 3497 (2021).
[54] Z. Tao, Q. Yu, S. Roy, and S. Hammes-Schiffer, Acc. Chem. Res. **54**, 4131 (2021).
[55] X. Xu and Y. Yang, J. Chem. Phys. **152**, 084107 (2020).
[56] X. Xu and Y. Yang, J. Chem. Phys. **153**, 074106 (2020).
[57] X. Xu, Z. Chen, and Y. Yang, J. Am. Chem. Soc. **144**, 4039 (2022).
[58] LONDON, a quantum-chemistry program for plane-wave/GTO hybrid basis sets and finite magnetic field calculations. By E. Tellgren (primary author), T. Helgaker, A. Soncini, K. K. Lange, A. M. Teale, U. Ekström, S. Stopkowicz, J. H. Austad, and S. Sen, See londonprogram.org for more information.
[59] Y. Yang, T. Culpitt, Z. Tao, and S. Hammes-Schiffer, J. Chem. Phys. **149**, 084105 (2018).
[60] T. Culpitt, Y. Yang, F. Pavošević, Z. Tao, and S. Hammes-Schiffer, J. Chem. Phys. **150**, 201101 (2019).
[61] E. Tellgren, T. Culpitt, L. Peters, and T. Helgaker, "Molecular vibrations in the presence of velocity-dependent forces," arXiv:2212.10246 (2022).
[62] T. Culpitt, L. D. M. Peters, E. I. Tellgren, and T. Helgaker, J. Chem. Phys. **156**, 044121 (2022).
[63] F. Tisseur and K. Meerbergen, SIAM Rev. **43**, 235 (2001).
[64] S. Sen and E. I. Tellgren, J. Chem. Phys. **148**, 184112 (2018).
[65] R. McWeeny, *Methods of Molecular Quantum Mechanics*, 2nd ed. (Academic Press, 1992).
[66] J. Olsen and P. Jørgensen, J. Chem. Phys. **82**, 3235 (1985).

[67]O. Christiansen, P. Jørgensen, and C. Hättig, Int. J. Quantum Chem. **68**, 1 (1998).
[68]P. L. Altick and A. E. Glassgold, Phys. Rev. **133**, A632 (1964).
[69]T. H. Dunning and V. McKoy, J. Chem. Phys. **47**, 1735 (1967).
[70]J. Broeckhove, L. Lathouwers, E. Kesteloot, and P. van Leuven, Chem. Phys. Lett. **149**, 547 (1988).
[71]T. Culpitt, Y. Yang, P. E. Schneider, F. Pavošević, and S. Hammes-Schiffer, J. Chem. Theory Comput. **15**, 6840 (2019).
[72]Y. Yang, P. E. Schneider, T. Culpitt, F. Pavošević, and S. Hammes-Schiffer, J. Phys. Chem. Lett. **10**, 1167 (2019).
[73]Q. Yu, F. Pavošević, and S. Hammes-Schiffer, J. Chem. Phys. **152**, 244123 (2020).
[74]C. C. Marston and G. G. Balint-Kurti, J. Chem. Phys. **91**, 3571 (1989).
[75]G. G. Balint-Kurti, C. L. Ward, and C. C. Marston, Comput. Phys. Commun. **67**, 285 (1991).
[76]S. P. Webb and S. Hammes-Schiffer, J. Chem. Phys. **113**, 5214 (2000).